J. Amer. Soc. Hort. Sci. 147(4):216–238. 2022. https://doi.org/10.21273/JASHS05189-22

Mapping Winterhardiness in Garden Roses

Cindy Rouet
Vineland Research and Innovation Centre, 4890 Victoria Avenue N, Lincoln, ON L0R 2E0, Canada; and University of Guelph, Plant Agriculture Department, 50 Stone Road E, Guelph, ON N1G 2W1, Canada

Joseph O'Neill and Travis Banks
Vineland Research and Innovation Centre, 4890 Victoria Avenue N, Lincoln, ON L0R 2E0, Canada

Karen Tanino
University of Saskatchewan, Department of Plant Sciences, 51 Campus Drive, Saskatoon, SK S7N 5A8, Canada

Elodie Derivry
APREL, Association Provençale de Recherche et d'Expérimentation Légumière, Route de Mollégès, 13210 Saint-Rémy-de-Provence, France

Daryl Somers
Somers Consulting, 521 Welland Road, Fenwick, ON LOS 1C0, Canada

Elizabeth A. Lee
University of Guelph, Plant Agriculture Department, 50 Stone Road E, Guelph, ON N1G 2W1, Canada

Additional index words. best linear unbiased predictors, black spot, cold hardiness, electrolyte leakage, freezing tolerance, heritability, quantitative trait loci, *Rosa* ×*hybrida*, woody perennials

Abstract. **Field winterhardiness is a critical trait in rose cultivars (*Rosa* ×*hybrida*) grown in northern climates. Although the molecular basis of cold hardiness has been well documented in model organisms such as *Arabidopsis thaliana*, little is known about the genetics and mechanisms underlying winterhardiness in roses. This research aims to explore the genetic control of winterhardiness for application in breeding programs using quantitative trail loci (QTL) analysis in two biparental rose populations derived from cold-hardy roses of the Canadian Explorer Series Collection. Field winterhardiness was assessed as a complex trait with winter damage and regrowth recorded in multiyear and multilocation trials in Ontario and Saskatchewan, Canada. In addition, this research explored the relationship between field measurements and electrolyte leakage recorded under artificial conditions. Electrolyte leakage had limited utility for application in rose breeding programs as a substitute for field evaluation, but did enable identification of QTL associated with potential cold hardiness candidate genes. A QTL for electrolyte leakage mapped to a genomic region that harbors a *CBF1*-like transcription factor. A total of 14 QTLs associated with field winter damage and regrowth were discovered, and they explained between 11% and 37% of the observed phenotypic variance. Two QTL associated with winter damage and regrowth overlapped with a known QTL for black spot (*Diplocarpon rosae*) disease resistance, *Rdr1*, in an environment under high disease pressure. Due to the complexity of field winterhardiness and its direct reliance on intertwined factors, such as overall plant health, moisture status, snow cover, and period of prolonged sub-zero temperatures, field trials are the ultimate measurement of field winterhardiness. Transgressive segregation was observed for all traits, and it was most likely due to complementary gene action. Field winter damage and regrowth were highly heritable in single environments, but they were subject to genotype × environment interaction resulting from pest pressure and severe climatic conditions.**

Received for publication 26 Jan. 2022. Accepted for publication 16 May 2022. Published online 12 July, 2022.
This work was supported by funding from the Vineland Research and Innovation Centre, Agriculture and Agri-Food Canada Growing Forward 2 project AIP-P013, Canadian Agricultural partnership, the Natural Sciences and Engineering Research Council of Canada (NSERC), the Ontario Ministry of Agriculture and Food (OMAFRA), the Canadian Nursery Landscape Association, Landscape Manitoba, and Landscape Alberta. The authors are grateful to the support of Dr. Parminder Sandhu for contributing to the development of the mapping populations, the International Tuition Scholarship from Ontario Agriculture College (OAC), and the technical support of Rensong Liu, Jackie Bantle, Ruobin Liu, and Gowribai Valsala (University of Saskatchewan). The authors also thank Peter Harris for his help unravelling the pedigree of RSM 104.
C.R. is the corresponding author. E-mail: rouetcindy@gmail.com.

Cold winters limit the cultivation of rose cultivars (*Rosa* ×*hybrida*) grown in northern climates and require rose cultivars that can survive prolonged periods of sub-zero temperatures. Different factors influence perennial crops' survivability, such as snow cover, moisture status, disease tolerance, insect damage, pathogen-induced defoliation, overall plant health, and environmental adaptation (Bélanger et al., 2006). Environmental adaptation includes dormancy and acquisition of maximum cold tolerance, which relies on the timing of acclimation and de-acclimation (Wisniewski et al., 2014). Most existing cultivars' climatic adaptability ranges are indicated by their U.S. Department of Agriculture (USDA) winterhardiness zone. Although most tender roses such as *Rosa chinensis* cultivars, hybrid tea roses, and floribunda roses are not able to withstand temperatures below −20 °C

(USDA cold hardiness zones 10 to 6), many shrub roses are able to withstand −45 °C (USDA cold hardiness zones 10 to 2).

Canadian-bred roses are known for their exceptional hardiness. Three prominent series of hardy roses supported by Agriculture and Agri-Food Canada were created between 1960 and 2016: the Explorer Series Collection, the Parkland Series, and the Canadian Artist Series. The Explorer Series Collection was initiated in the 1960s in Ottawa, ON, Canada, via interspecific crosses from rose species *R. chinensis, Rosa wichurana, Rosa rugosa, Rosa ×kordesii, Rosa laxa, Rosa spinossisima*, and *Rosa acicularis* (Svejda, 2008). The roses from this collection are rather winter hardy, as most can survive severe winter conditions and show good spring regrowth. The Parkland Series of roses can survive cold winters, provided that they are protected by snow cover, but most generally die back to the snow line or to the crown, expressing different strategies of winter survival and environmental adaptation in comparison with the Explorer Series of roses. The Canadian Artist roses are a subsequent series after the breeding programs of the Explorer and Parkland Series of roses closed and are derived from breeding lines generated by both programs. More recently, the 49th Parallel Collection series represents the latest effort supported by Vineland Research and Innovation Centre (Vineland, ON, Canada) to release hardy roses for northern climates.

Although cold hardiness is overall considered as a multigenic trait (Guy, 1990; Wisniewski et al., 2014), the trait in roses is thought to be controlled by a few major genetic factors and to be highly heritable (Svejda, 1979). As a result, large gains from selection can be made when hybridizing hardy parental genotypes (Zlesak, 2007). A recent QTL mapping study suggested the potential existence of a major QTL for cold hardiness in the genetic background of roses from the Explorer Series on linkage group 5, which also displayed the highest genetic differentiation between Canadian and European-bred roses (Vukosavljev, 2014). However, this QTL was not validated. Further efforts are needed toward the identification of robust QTL for winterhardiness in roses to improve the efficiency of breeding schemes through the development of molecular markers and the pyramiding of these QTL in elite roses.

The power and robustness of QTL detection and the development of new genomic tools rely on the experimental design and the accuracy of phenotyping; however, winterhardiness is a complex trait that is difficult to define and assess. The ability to accurately assess a genotype's true winterhardiness is challenging, as it is affected by many abiotic and biotic factors and a successful acclimation. Although winterhardiness in roses has been traditionally evaluated in the field on an ordinal scale based on the overall level of damage observed after several winters across multiple locations (Svejda, 1979), cane dieback and spring regrowth are all components of field winterhardiness that need to be considered together and recorded separately (Zlesak., et al., 2017). Freezing tolerance is a trait of important agronomic interest (Gery et al., 2011), and screening methods under artificial conditions for freezing tolerance would complement field-screening approaches for QTL detection. Plant electrolyte leakage, which is a measurement of membrane damage after subjecting a plant organ to freezing treatment, has been successfully used as an index of freezing tolerance for various crops, such as alfalfa [*Medicago sativa* (Dexter et al., 1930)], winter wheat [*Triticum aestivum* (Săulescu and Braun, 2001; Willick et al., 2019)], durum wheat [*Triticum durum* (Bajji et al., 2002)], walnut [*Juglans regia* (Poirier et al., 2010)], pea [*Pisum sativum* (Dumont et al., 2009)], red raspberry [*Rubus idaeus* (Lindén et al., 2000)], switch grass [*Panicum virgatum* (Peixoto and Sage, 2016)], silver grass [*Miscanthus sacchariflorus*, *Miscanthus sinensis* (Peixoto and Sage, 2016)], hybrid poplar [*Populus* sp. (Kalcsits et al., 2009)], and on a limited number of rose cultivars (Karam and Sullivan 1991; Le et al., 2012; Ouyang et al., 2019). Therefore, electrolyte leakage has the potential to be used in QTL mapping as a quantitative and objective measurement of frost damage for application in a rose breeding program to select for freezing tolerance and minimal cane dieback without the need for field screening.

Although the genetics of cold hardiness remains poorly understood in roses, it has been well documented in model organisms such as *Arabidopsis thaliana.* In temperate regions, the perception of the cold signal at the early stage of acclimation induces a cascade of changes in gene expression and metabolism pathways that leads to the acquisition and the support of cold hardiness (Akhtar et al., 2012). For instance, cold-induced metabolic changes in roses include a decrease in starch content, an increase in oligosaccharides, and an increase in sucrose content in the cells (Ouyang et al., 2019). At the genetic level, the C-repeat binding factor (CBF)-dependent responsive pathway is known to play a critical role in the acquisition and regulation of plant cold hardiness in *A. thaliana* (Novillo et al., 2007). Part of the *CBF* pathway is thought to be conserved among plant species, but the regulation of *CBF* genes is more complex in woody perennials than in herbaceous plants (Wisniewski et al., 2014). The expressions of a few *CBF/DREB*-like proteins have been studied in various Rosaceae crops, such as peach [*Prunus persica* (Wisniewski et al., 2011)], almond [*Prunus dulcis* (Barros et al., 2012)], sweet cherry [*Prunus avium* (Kitashiba et al., 2004)], and Japanese plum [*Prunus mume* (Zhao et al., 2018)], so it is reasonable to assume that these proteins are present in roses as well. Most of the QTL involved in freezing tolerance in *A. thaliana* are in the *CBF* gene regions or nearby (Gery et al., 2011), highlighting the important role of the *CBF* pathway in the acquisition of cold hardiness and setting up a framework for the identification of candidate genes in linkage mapping research.

The aim of this research was to provide rose breeders with the necessary tools to develop winter-hardy roses most efficiently. The objectives were to 1) investigate the utility of electrolyte leakage as a measure of cold hardiness in rose breeding material, 2) measure electrolyte leakage in two mapping populations with different levels of winterhardiness and identify QTL associated with electrolyte leakage, 3) conduct multiyear multilocation field trials to measure winter damage and regrowth in the same two mapping populations and identify QTL for regrowth and winter damage, and 4) compare winterhardiness data inferred by both electrolyte leakage and field screening in the breeding material.

Materials and Methods

This study comprised three complementary experiments: 1) electrolyte leakage experiments on a small set of commercial and elite roses (Expt. 1); 2) electrolyte leakage experiments on the parental genotypes and large-scale electrolyte leakage experiments on two mapping populations with QTL mapping of electrolyte leakage (Expt. 2); and 3) multiyear, multisite

winterhardiness field trials with QTL mapping for field winter damage and spring regrowth (Expt. 3).

Expt. 1: Electrolyte leakage as a proxy for winterhardiness

Genetic material. A set of 28 roses consisting of eight elite roses from the Vineland Research and Innovation Centre's (VRIC, Vineland, ON, Canada) breeding program, one breeding line (CA60), and 19 commercial rose cultivars that were a mixture of roses from the Explorer Series (George Vancouver, John Cabot, John Davis, John Franklin, Lambert Closse, Martin Frobisher, Quadra, William Baffin, William Booth), floribunda [KORmuse (Salmon Vigorosa), MACivy (Singin in the Rain), Poseidon (Novalis)], hybrid tea [MEInomad (Desert Peace), MEIpierar (Caroline de Monaco), Peace, WEKrigoyelo (Gentle Giant)], grandiflora [MEImouslin (Cardinal Song)], and shrub roses [BAIine (Yellow Submarine), RADrazz (Knock Out)], and that varied in their level of winterhardiness (Table 1) were used in this experiment. All the roses were grown on their own roots.

Experimental design and growing conditions. The plants were propagated from cuttings in early-Winter 2016 using foam strips designed for vegetative propagation of cuttings (Oasis strips; Oasis Grower Solutions, Kent, OH) in the mist house, potted into 7.5-L pots (22 cm height, 22 cm width) in a soilless potting mix (Sunshine Mix 1; Sun Gro Horticulture, Agawam, MA) and grown outdoors. Roses were manually watered daily and fertilized two to three times per week with 20N–3.4P–16.6K and 14N–0P–11.6K fertilizers (Plant-Prod; Master Plant-Prod Inc., Brampton, ON, Canada) at an electrical conductivity (EC) level in the range of 1.2 to 1.6 $dS \cdot m^{-1}$.

The electrolyte leakage assay consisted of three main steps: 2 weeks' acclimation of whole plant at 4 °C, freezing treatment of stem segments from acclimated plants, and measurement of conductivity before and after autoclaving of the stem segments. Expt. 1 was replicated between one and three times depending on the genotype (i.e., replications in time) using unique sets of clones for each replication (i.e., true biological replications) (Supplemental Table 1), and it was conducted from May to Aug. 2016.

In addition, 12 of the commercial rose cultivars used in electrolyte assays were planted in 2017 in the field at VRIC (lat. 4311'30.9″N, long. 7923'45.7″W; cultivated Gleyed Brunisolic Gray Brown Luvisol soil with sandy loam) using a completely random design (CRD) with three replications. The 12 cultivars were grown on the rootstock *Rosa multiflora*. Plants were spaced by 50 cm within rows, and the rows were spaced by 1.50 m. The eight elite roses were planted on their own roots according to CRD with six replications in 2013 in Saskatoon, SK, Canada, and Olds, AB, Canada, as part of the Pan Canadian testing, a network of growers and university partners across Canada who evaluate VRIC's selected roses.

Phenotyping. The experiment was conducted according to Dexter et al. (1930) with various modifications to the authors' original protocol. After the acclimation period, rose stems from acclimated plants were collected, sprayed with type 1 water (Milli-Q; Merck KGaA, Darmstadt, Germany) to nucleate ice formation, and placed into sealable plastic bags. The bags were moved to a programmable freezer in which the temperature dropped from 0 to −20 °C, at a rate of $-2.5\,°C \cdot h^{-1}$. One stem per genotype was removed from the freezer at 0, −5, −10, −15, and −20 °C. The stem removed from the freezer was then cut into 10 1-cm-long stem sections and each section placed into individual 20 mL centrifuge tubes filled with type 1 water (i.e., technical replications). The tubes were shaken overnight at a relatively low speed in a benchtop orbital shaker before conductivity was measured and recorded as R_0 using a traditional EC meter with a probe (Oakton CON 450; Cole-Parmer Instrument Co., Montreal, QC, Canada). The tubes were then autoclaved for 1 h at 120 °C to promote cell rupture and shaken again overnight. Conductivity was measured again and recorded as R_t. The percentage of electrolyte leakage (EL) was calculated as follows: $EL\ (\%) = 100 \times \frac{Ro}{Rt}$. In addition, field winterhardiness was recorded on a scale from 0 to 5 (0 = no winter damage, 1 = damage on the tips of the canes only, 2 = damage down to the snow line, 3 = damage to the crown with good spring regrowth, 4 = damage to the crown with poor spring regrowth, 5 = dead plant) in Spring 2018 (VRIC) for the 12 commercial rose cultivars, and in the Spring of 2014 and 2015 (Alberta and Saskatchewan) for eight elite roses.

Data analysis. The percentage of electrolyte leakage was averaged for up to three replications for each cultivar (Supplemental Table 1). The lethal temperature at which 50% of leakage occurred (LT50) was estimated using a logistic regression on electrolyte leakage data according to the formula: $\ln\left(\frac{L}{1-L}\right) = a + bX$, where L was the proportion of electrolyte leakage corrected for leakage not due to freezing (i.e., control) and X was the logarithm to base 10 of the temperature. Correlations among electrolyte leakage, LT50, field data, and USDA cold hardiness zone were computed using the Pearson method in the RStudio software (RStudio Team, Boston, MA).

Expt. 2: QTL mapping of electrolyte leakage

Genetic material. Two mapping populations and their parental genotypes grown on their own roots were used in this experiment (Table 1). The first mapping population was a tetraploid F_1 rose population created between 2015 and 2016 from the cross between the cold-hardy female parent CA60 and the cold-susceptible male parent Singin' in the Rain ('SITR'). The cold-hardy female CA60 originated from the Morden rose breeding program from a cross between RSM 104 and the cold-hardy Canadian Explorer rose 'Frontenac' (Ogilvie, 1993). The female parent RSM 104, also named 91/104–1, was a German selection resulting from a cross between CT50–9 (a chromosome doubled clone of 88/124–46, which was selected in 1987 and sawn in 1988) and the cultivar TANca (Caramba). The diploid genotype 88/124–46 is the product of selection after three generations of open pollination from a cross of a tetraploid cultivar (most probably Taunusblümchen) with an *R. multiflora* selection (T. Debener, personal communication). CA60 has demonstrated exceptional winterhardiness in the field at Vineland, ON, Canada. The second mapping population consisted of 107 individuals and resulted from the 2016-cross between the cold-susceptible female parent 'HARpageant' [Easy Does It ('EDI')] and the cold-hardy male parent 'George Vancouver' ('GV'). 'GV' was bred by Felicitas Svejda and belongs to the Explorer Rose Collection.

Experimental design and growing conditions. The plants from the CA60 × 'SITR' population and its parents were propagated from cuttings between Aug. 2017 and Jan. 2018, and the plants from the 'EDI' × 'GV' population and its parents were propagated from Jan. to Mar. 2019. The propagation was staggered over a few months to manage a variable rooting success rate, but the age of each cutting was not recorded. The cuttings were propagated in a mist house directly into a soilless potting

Table 1. Genetic material used in the genetic mapping of electrolyte leakage and field winterhardiness of garden roses (*Rosa* ×*hybrida*).

Genotype	USDA zone[z]	Ploidy[y]	Type
Expt. 1: Electrolyte leakage as a proxy for winterhardiness[x]			
Cardinal Song (‘MEImouslin’)	7b	Unknown	Grandiflora
Caroline de Monaco (‘MEIpierar’)	7b	Unknown	Hybrid tea
Desert Peace™ (‘MEInomad’)	7b	Unknown	Hybrid tea
Gentle Giant™ (‘WEKrigoyelo’)	6b	Unknown	Hybrid tea
‘George Vancouver’ (‘GV’)	3b	4x	Hybrid Kordesii. Explorer Series Collection
‘John Cabot’	2b	4x	Hybrid Kordesii. Explorer Series Collection
‘John Davis’	2b	3x	Hybrid Kordesii. Explorer Series Collection
‘John Franklin’	3b	4x	Hybrid Spinosissima. Explorer Series Collection
Knock Out (‘RADrazz’)	4b	3x	Shrub rose
‘Lambert Closse’	2b	4x	Shrub (floribunda × *R.* ×*kordesii*). Explorer Series Collection
‘Martin Frobisher’	2b	2x	Hybrid Rugosa. Explorer Series Collection
‘Peace’	5b	4x	Hybrid tea
Novalis® (‘Poseidon’)	5b	Unknown	Floribunda
‘Quadra’	3b	Unknown	Hybrid Kordesii. Explorer Series Collection
Salmon Vigorosa (‘KORmuse’)	5b	Unknown	Floribunda
Singin’ in the Rain [‘SITR’ (‘MACivy’)]	6b	Unknown	Floribunda
‘William Baffin’	2b	4x	Hybrid Kordesii. Explorer Series Collection
‘William Booth’	2b	4x	Hybrid Kordesii. Explorer Series Collection
Yellow Submarine™ (‘BAIine’)	4b	Unknown	Shrub
S13–10		Unknown	Elite rose from VRIC
S13–29		Unknown	Elite rose from VRIC
S13–3		Unknown	Elite rose from VRIC
S13–32		Unknown	Elite rose from VRIC
S13–35		Unknown	Elite rose from VRIC
S13–6		Unknown	Elite rose from VRIC
S13–7		Unknown	Elite rose from VRIC
S13–8		Unknown	Elite rose from VRIC
CA60		Unknown	Explorer-derived hybrid
Expt. 2: QTL mapping of electrolyte leakage			
CA60		Unknown	Explorer-derived hybrid
‘SITR’	6b	Unknown	Floribunda
Easy Does It [‘EDI’ (‘HARpageant’)]	5	Unknown	Floribunda and hybrid tea
‘GV’	3b	4x	Hybrid Kordesii. Explorer Series Collection
CA60 × ‘SITR’ population		Unknown	
‘EDI’ × ‘GV’ population		Unknown	
CA60		Unknown	Explorer-derived hybrid
‘SITR’	6b	Unknown	Floribunda
Expt. 3: QTL mapping of field-based winterhardiness			
CA60 × ‘SITR’ population		Unknown	
‘EDI’ × ‘GV’ population		Unknown	
Caroline de Monaco	7b	Unknown	Hybrid tea
‘Frontenac’	2b	4x	Hybrid Kordesii. Explorer Series Collection
Gentle Giant	6b	Unknown	Hybrid tea
‘Nicolas’	3b	4x	Shrub. Explorer Series Collection
‘EDI’	5	Unknown	Floribunda and hybrid tea
‘GV’	3b	4x	Hybrid Kordesii. Explorer Series Collection
CA60		Unknown	Explorer-derived hybrid
‘SITR’	6b	Unknown	Floribunda

[z]The cultivars, elite roses, and parental lines differ in their U.S. Department of Agriculture (USDA) cold hardiness zones (1–13 scale); a rose adapted to zone 2b being the hardiest in this list.

[y]x represents the basic complete set of chromosomes; most of the roses in this study are tetraploid (4x).

[x]This research used three experiments (Expt. 1–3). Although Expt.1 used a set of different commercial cultivars and elite roses from the Vineland Research and Innovation Centre’s (VRIC, Vineland, ON, Canada) rose breeding program, Expts. 2 and 3 focused on two mapping populations with the parental genotypes CA60, ‘EDI’, ‘SITR’, and ‘GV’.

mix (Sungro Sunshine Mix 1) or using foam strips. The mist house was heated at 22 °C; the temperature varied between 20 and 25 °C but rose to 35 °C during the hottest summer months. The relative humidity was between 60% and 75% and the misting system was activated every 5 min during a 16 h photoperiod. High-pressure sodium (HPS) supplemental light was provided to maintain a 16 h photoperiod. Cuttings were transferred into 0.5-L pots (9.5 cm height, 10 cm width) between 2 and 4 weeks after propagation before being transplanted into 11-L pots (24 cm height, 25 cm width). Roses were kept in 0.5-L pots (9.5 cm height, 10 cm width) for a minimum time of 4 weeks before being transplanted into larger pots. Plants from the CA60 × 'SITR' population were grown on their own roots and maintained in the greenhouse from Sept. 2017 to Oct. 2018. Temperature in the greenhouse was maintained at an average of 24 °C, but diurnal variation of temperature occurred with a maximum–minimum temperature range of 30/18 °C (day/night); 400-W HPS supplemental light was provided from Oct. 2017 to May 2018 to maintain a 16-h photoperiod. Plants from the 'EDI' × 'GV' population were grown on their own roots and maintained outdoors from May to Oct. 2019 because of restricted space in the greenhouse. Average outdoor temperature in 2019 varied from 12 °C in May, 23 °C in the hottest summer months, and 12 °C in October. All plants were watered with the use of irrigation strips and fertilized two to three times per week with 20N–3.4P–16.6K and 14N–0P–11.6K fertilizers (Plant-Prod) at EC level in the range of 1.2 to 1.6 $dS{\cdot}m^{-1}$. Only sulfur was applied to control powdery mildew on the plants, no additional chemicals were used. Biocontrol was used to control insect pressure.

A total of 100 genotypes from the population CA60 × 'SITR' and 88 from the population 'EDI' × 'GV', in addition of the parental genotypes CA60, 'SITR', 'EDI', and 'GV', were used in electrolyte leakage experiments. In preparation for the electrolyte leakage experiments, the plants from each mapping population were moved to a greenhouse maintained at an average temperature of 10 °C (i.e., pre-acclimation phase) where diurnal variation of temperature occurred with a maximum–minimum temperature range of 25/8 °C (day/night) with dark for 16 $h{\cdot}d^{-1}$ and shading as needed and without supplemental light or fertilization. Plants were then subjected to a 2-week artificial acclimation period in a walk-in cooler at 4 °C (KeepRite Refrigeration, Brantford, ON, Canada) in which two light-emitting diode (LED) tripods [Husky Model DE007; Stanley Black & Decker (Mississauga, ON, Canada); Western Forge (Colorado Springs, CO); Apex Tool Group (Sparks, MD); and Iron Bridge Tools (Shelburne Falls, MA)] and two 30-m metal cage string lights with LED bulbs (E253217 Model LS-100; Ningbo Linsheng Electric Co., Ltd., Zhejiang, China) delivered 10 $\mu mol{\cdot}m^{-2}{\cdot}s^{-1}$ of light at canopy level for 6 $h{\cdot}d^{-1}$. Photosynthetically active radiation was determined from quantum sensors (LI-250A; LI-COR, Lincoln, NE). Clones of the F_1 progeny were brought to the cooler over several weeks to conduct multiple replications of the experiments as detailed in the following paragraph, and the plants were randomized in the cooler using the online plant breeding platform Phenome (Phenome Networks Ltd, Rehovot, Israel). Sections that were 10 cm long and of similar diameter were collected at the proximal end of the stem (i.e., experimental unit) from acclimated plants and were subjected to freezing treatments in a programmable freezer. This experiment used a split-plot design in which temperature represented the main-plot factor and genotypes were assigned to the subplots.

Electrolyte leakage experiments on the parental lines, the population CA60 × 'SITR' and the population 'EDI' × 'GV' were conducted separately. Experiments on the parental lines were conducted in Nov. 2019 and replicated three times with unique sets of clones (i.e., true biological replications) with three stem sections per genotype and temperature (i.e., technical replications) and 1 week between each replication (i.e., replications in time). A fourth replication was conducted on CA60 and 'GV' only, using a distinct set of clones 2 weeks after the third replication. Clones of the parental genotypes were moved to the pre-acclimation house in Oct. 2019. Experiments on the population CA60 × 'SITR' were conducted from Nov. 2018 to Jan. 2019 and replicated five times (i.e., replications in time) using five stem sections per temperature and per genotype (i.e., technical replications) and three unique sets of clones (i.e., true biological replications), two of which were used in two replications and were allowed to de-acclimate in a greenhouse at room temperature for 2 weeks before being reused. There were 2 weeks between each replication, with the exception of 3 weeks between replications 3 and 4. Plants from the CA60 × 'SITR' population were moved to the pre-acclimation house in Oct. 2018. Experiments on the population 'EDI' × 'GV' were conducted from Jan. to Feb. 2020 and replicated three times (i.e., replications in time) with unique sets of clones (i.e., true biological replications), with 2 weeks between each replication. Only one stem section per temperature and genotype was used in the experiment on the 'EDI' × 'GV' population. Plants from the 'EDI' × 'GV' population were moved to the pre-acclimation house in Oct. 2019.

Phenotyping. The electrolyte leakage assay was conducted as described in the previous section (Expt. 1: Electrolyte leakage as a proxy for winterhardiness) with some modifications. The bags containing the rose stems were moved to a programmable freezer in which the temperature dropped from 0 to −50 °C (experiments on the parental lines), from 0 to −20 °C (experiments on the population CA60 × 'SITR') and from 0 to −40 °C (experiments on the population 'EDI' × 'GV'), at a rate of $-2.5\ °C{\cdot}h^{-1}$, with a 12-h nucleation step at −4 °C. The initial stem from the sealable plastic bag that was taken out of the freezer was then cut into three, five or one 1-cm-long stem sections in the experiments conducted on the parental lines, the population CA60 × 'SITR' and the population 'EDI' × 'GV', respectively. The stem sections were cut in a way that excluded buds and thorns. Each section was placed into individual 5-mL centrifuge tubes filled with type 1 water (i.e., technical replications). R_0 and Rt were recorded before and after autoclave as described previously using a compact EC meter (LAQUAtwin-EC-11; Horiba, Ltd., Kyoto, Japan) with 120 μL of solution. Data on the parental lines were recorded at 4 (i.e., control), −10, −15, −20, −25, −30, −35, −40, −45, and −50 °C; data on the population CA60 × 'SITR' were recorded at −10, −15, and −20 °C; and data on the population 'EDI' × 'GV' were recorded at 4 (i.e., control), −10, −15, −20, −25, −30, −35, and −40 °C. The percentage of electrolyte leakage was calculated as described previously. In addition, an index of injury (I) corrected for electrolyte leakage not due to freezing—measured at 4 °C—was estimated for the parental genotypes and the population 'EDI' × 'GV' by the formula $I\ (\%) = \frac{\frac{R0}{Rt} - \frac{Roref}{Rtref}}{1 - \frac{Roref}{Rtref}}$ as described by Ouyang et al. (2019).

Data analysis. The analysis was conducted separately for the parental lines, the population CA60 × 'SITR', and the

population 'EDI' × 'GV'. Generalized linear mixed models (GLMM) were fitted to the electrolyte leakage data using SAS software (SAS version 9.4; SAS Institute Inc., Cary, NC), specifying a beta distribution and the logit link under the GLIMMIX procedure (Supplemental Material). Temperature was a fixed effect. Genotypes were considered as fixed effects when analyzing only the parental lines, and the best linear unbiased estimates (BLUE) were computed. Genotypes were considered as random effects in the analysis of the mapping populations, and the best linear unbiased predictors (BLUP) were computed. In addition, LT50 was estimated for the parental lines CA60, 'SITR', 'EDI', and 'GV' by fitting a nonlinear regression dosage curve response on the index of injury with nine temperatures (−10, −15, −20, −25, −30, −35, −40, −45, and −50 °C), using the nlmixed procedure in the SAS software. In the same way, LT50 was estimated individually for each sibling of the 'EDI' × 'GV' population, from the index of injury obtained from six temperatures (−15, −20, −25, −30, −35, and −40 °C). The index of injury was used to compute the LT50s; the BLUPs of electrolyte leakage and the LT50 were used in QTL mapping.

The female and male genetic maps of CA60 and 'SITR' were created from data previously generated through genotyping by sequencing [GBS (Rouet et al., 2019)] to include all individuals for which cold hardiness data were available. The female and male maps of 'EDI' and 'GV', respectively, were created from newly generated GBS data following a two-way pseudo-test cross-mapping strategy, using R-package ASMap (Taylor and Butler, 2017), as described by Li et al. (2014) and applied on roses in Rouet et al. (2019). The four parental genetic maps were used as a framework for QTL mapping. A total of 83 and 80 individuals were used to identify QTL associated with electrolyte leakage from the CA60 × 'SITR' and 'EDI' × 'GV' populations, respectively. For the 'EDI' × 'GV' population, 76 individuals were also used to identify QTL associated with LT50.

QTL were initially detected by interval mapping (IM) using the R/qtl2 package (Broman et al., 2019) and performing a genome scan by Haley-Knott regression (Haley and Knott, 1992). Then, results from IM were compared with a multiple QTL mapping (MQM) approach using the R implementation of Ritsert Jansen's MQM method (Arends et al., 2010) (R version 3.5.3; R Foundation for Statistical Computing, Vienna, Austria), and additional QTL were detected. Both forward stepwise and backward elimination strategies were used to identify QTL underlying the trait in MQM. The forward stepwise approach was conducted by setting the major QTL detected in IM as cofactors. Variance components used in QTL modeling were estimated by the restricted maximum likelihood (REML) approach. Significance cutoff was determined by performing 1000 permutations and the fitqtl function from the package R/qtl (Broman et al., 2003) was applied to estimate the percentage of variation explained by the main QTL. Bayes intervals were obtained with 95% confidence for the QTL. Only the results from MQM were reported. The relative position of the single-nucleotide polymorphism (SNP) markers in the reference genome *R. chinensis* 'Old Blush' V2 were used to identify QTL intervals.

Expt. 3: QTL mapping of field-based winterhardiness

Genetic material. The two mapping populations described previously, CA60 × 'SITR' and 'EDI' × 'GV', and their parental lines were used in this experiment. For both populations, the genotypes used in field trials overlapped with the genotypes used in electrolyte leakage experiments. In addition, four cultivars that were a mixture of hybrid teas and roses from the Explorer Series were used as controls in this experiment: cold-sensitive cultivars MEIpierar (Caroline de Monaco) and WEKrigoyelo (Gentle Giant), and cold-hardy cultivars Frontenac and Nicolas (Table 1). The mapping populations were grown on their own roots. The parental lines 'SITR' and 'EDI', and the controls were obtained from a local nursery and grown on *R. multiflora* rootstock. The parental genotype 'GV' was grown both on its own roots and grafted on *R. multiflora* rootstock (Table 1).

Experimental design and growing conditions. The population CA60 × 'SITR' was propagated from cuttings using foam strips in the mist house between Aug. 2017 and Jan. 2018 at the same time as the cuttings intended for electrolyte leakage experiments. The propagation was staggered over a few months to manage a variable rooting success rate, but the age of each cutting was not recorded. A total of 101 F_1 progeny and nine control and parental genotypes were planted in two locations in Canada in early June 2018: Elora, ON, Canada (lat. 43°38'27.4″N, long. 80°24'03.2″W; USDA zone 5b; cultivated Brunisol soil with silt loam) and Saskatoon, SK, Canada (lat. 52°07'21.5″N, long. 106°36'41.8″W; USDA zone 3b; Dark Brown Chernozemic soil). Roses were planted at each location using a randomized complete block design (RCBD) with five replications designed with the online plant breeding platform Phenome, the experimental unit being the rose bush. Plants were spaced by 60 cm within rows, and the rows were spaced by 1.50 m. Black heavy duty woven polypropylene landscape fabric and 46,000 kg of organic light-colored mulch, which was applied on top of the landscape fabric, were used to control weeds in Elora, and only mulch was used in Saskatoon. Plants were pruned in Summer 2019 to remove all the dead canes. The population 'EDI' × 'GV' was propagated from cuttings into a soilless potting mix in the mist house from Jan to Mar. 2019 at the same time as the cuttings intended for electrolyte leakage experiments. A total of 96 F_1 progeny and four parental genotypes were planted in late July. 2019 in Elora using an RCBD with three replications. Plants were spaced by 1 m within rows to accommodate their spreading architecture, and the rows were spaced by 1.50 m. Organic light-colored mulch was used to control weeds. The population CA60 × 'SITR' was assessed over two seasons (Winters 2019 and 2020), and the population 'EDI' × 'GV' was assessed over only one season (Winter 2020). In addition, climate data for Saskatoon were retrieved from the Saskatchewan Research Council Website at the Saskatoon Climate Reference Station (Saskatchewan Research Council, 2021), and climate data collected at the Elora Research Station were retrieved from the Environment Canada Website (Environment Canada, 2021).

Phenotyping. Field winterhardiness was assessed as two components: winter damage and spring regrowth as described by (Vukosavljev, 2014). Winter damage was a measurement of cane dieback using the following formula: $\mathrm{WD}\ (\%) = 100 \times \frac{ld}{lt}$ with WD being the percentage of winter damage, ld the length of dieback and lt the length of the whole cane. Three stems per plant were measured and the average value for each plant was used as the rating for winter damage. Regrowth was estimated with the following formula: $\mathrm{RG}\ (\%) = 100 \times \frac{ln}{lt}$, with RG being the percentage of regrowth, ln the length of the new shoot, and lt the initial length of the whole cane. Regrowth value for each genotype was calculated as the average regrowth of three branches. For both winter damage and regrowth, the

three longest stems from the crown were chosen. Therefore, the height of the three tallest stems that were emerging in the spring were used in reference to the overall height of the three tallest stems going into the previous winter to estimate regrowth. The number of newly emerging shoots from multiple axillary buds was not recorded.

Winter damage was measured in early spring when the leaf buds started to grow actively. Spring regrowth was measured during the second week of June 2019 and first week of July 2020 in Elora and during the last week of July 2019 and 2020 in Saskatoon. Plants that died through Winter 2019 were assigned 100% winter damage for Winter 2019 and missing data for winter damage 2020, regrowth 2019, and regrowth 2020. Plants that died in Spring 2019 because of planting, drought, or pest pressure were assigned missing data for winter damage and regrowth across years. Plants that died through the Winter 2020 were assigned 100% winter damage in 2020 and missing data for regrowth 2020. This was done to ensure that the timing of a plant's death was accurately captured and that the ability of the meristem to resume growth in the spring even on highly damaged plants was well represented. Winter damage and regrowth data were collected in Elora in 2019 and in 2020 and in Saskatoon in 2019 and in 2020 for the population CA60 × 'SITR' and in Elora in 2020 for the population 'EDI' × 'GV'. Pest-induced defoliation [black spot (*Diplocarpon rosae*), rose slugs (*Endelomyia aethiops*), and sawflies (Hymenoptera)] was also recorded in Sept. 2019 in Elora on a scale from 0 to 4 (0 = no defoliation and intact leaves, 1 = minor damage to the leaves mainly caused by caterpillars, 2 = minor defoliation with leaves left all over the rose bush, 3 = leaves left only on the tips of the stems, 4 = no leaves left, severe defoliation).

Data analysis. Descriptive statistical analyses were first conducted on field data for the two mapping populations using the RStudio software. The data were then modeled with a three-dimensional productivity contour map using SAS software (version 9.4) and the spline method in the G3GRID procedure to investigate the presence of nonrandom error distribution. A GLMM was fitted to field data using the SAS software, and the GLIMMIX procedure was used to conduct a genotype × environment (GE) interaction analysis with up to four environments (Elora 2019, Elora 2020, Sask 2019, Sask 2020). The variances of regrowth and winter damage for the field trial CA60 × 'SITR' with multiple environments were partitioned into random effects genotype, environment, GE, and block (environment). When analyzing environment separately, the variances of regrowth and winter damage for the field trial 'EDI' × 'GV' and the field trial CA60 × 'SITR' were partitioned into random effects: Block and Genotype. The linear predictors were respectively: $\eta_{ij} = \eta + E_i + a_j + (Ea)_{ij} + b(E)_{ki}$, where η was the intercept, E_i the environment effect, a_j the genotype effect, $(Ea)_{ij}$ the GE interaction, and $b(E)_{ki}$ the bloc effect nested within environment, and $\eta_{ij} = \eta + b_i + a_j$, where η was the intercept, a_j the genotype effect, and b_i the block effect. A type I error of 0.05 was used to determine the significance of tests in this analysis. Random effects were assessed with a likelihood test for covariance parameters. Winter damage data across environments and from single environments Elora 2020 and Sask 2019 were fitted to a beta distribution with a logit link function and Laplace interval estimation method. Winter damage data from single environments Elora 2019 were fitted to a normal distribution with the identity link function. Regrowth data were fitted to a lognormal distribution with the identity link function. The best fitted model was chosen based on the analysis of residuals and the fit statistics such as the AIC. The models were surveyed to determine if setting a heterogeneous covariance structure was necessary. BLUP estimates were computed for each genotype in each environment.

Heritability estimates were obtained for each trait in single environments by estimating the genetic variance components from the completely random mixed model. In the case in which the data fitted a normal or lognormal distribution in a completely random model, REML was used to compute and retrieve the variance estimates. Broad sense heritability used the following equation: $H^2 = \frac{Vg}{Vg + \left(\frac{Vr}{r}\right)}$, where H^2 was the broad sense heritability, V_g the genetic variance, V_r the residual variance, and r the number of replicates or blocs in the RCBD trial (Gitonga et al., 2014). Broad sense heritability was obtained from REML-derived estimates whenever the data were about normally distributed, as advised by Nakagawa and Schielzeth (2010). However, if the data fitted a beta distribution with a logit link function, the latent-scale heritability was obtained from the GLMM-based estimates (Nakagawa and Schielzeth, 2010). Under this scenario, the residual variance was calculated as follows: $Vr = \phi + \frac{\pi^2}{3}$, where ϕ was the scale parameter computed by the GLMM and represented the over dispersion of the data under the latent scale, and $\frac{\pi^2}{3}$ represented the variance for the logistic distribution. The latent-scale broad sense heritability was calculated by the following formula: $H^2 = \frac{Vg}{Vg + \left(\frac{\phi + \frac{\pi^2}{3}}{r}\right)}$. In addition, the ratio $\frac{Vge}{Vg}$ was calculated to quantify the size of the GE interaction relative to the genetic variance in mixed models using multiple environments (Gitonga et al., 2014).

Environment-metric preserving genotype plus GE interaction (GGE) biplots were generated using the BLUPs of field winter damage and regrowth to visually characterize simultaneously genotype by environment relationships using RStudio and the packages GGEBiplot GUI (Frutos et al., 2014). The GGE-biplot model uses the principle of singular value decomposition (SVD) to decompose genotype (G) and GE effects into two or more components represented on the graph axis. GGE-biplots were generated using the column metric preserving option (SVP = 2), tester-centered (Center = 2) and unscaled G + GE (Ling et al., 2021). BLUPs of winter damage and regrowth were also used in QTL mapping. A total of 83 and 86 individuals were used to identify QTL in the population CA60 × 'SITR' and in the population 'EDI' × 'GV', respectively. The presence of QTL was investigated and reported as previously described (Expt. 2: QTL mapping of electrolyte leakage). Finally, pathogen-induced defoliation data recorded in Elora in 2019 were averaged for each genotype across five blocks and used in correlation analysis with BLUPs of winter damage and regrowth and in mapping. Climate data were visualized in RStudio using the package ggplot2 (Wickham, 2016). The monthly number of freeze-thaw cycles were calculated as the number of days where the maximum temperature was higher than 0 °C and the minimum temperature was below −1 °C.

Relationship between electrolyte leakage and field winterhardiness. Correlations between the BLUEs and the BLUPs of electrolyte leakage and index of injury, LT50, and field data were computed using the Pearson method in the RStudio software.

Results

Expt. 1: Electrolyte leakage as a proxy for winterhardiness

Electrolyte leakage experiments conducted on 28 commercial cultivars and elite genotypes to investigate the relationship between electrolyte leakage and field winterhardiness on a small scale showed positive correlations between the different variables. Two of the genotypes ('Martin Frobisher' and 'William Booth') were inconsistent in their blooming patterns and were removed from the analysis due to concerns about correct identity. The USDA cold hardiness zone of the remaining cultivars was highly correlated with field winterhardiness (Fig. 1). In addition, the percentage of electrolyte leakage at −15 and −20 °C was strongly correlated with field winterhardiness and with the USDA cold hardiness zone (Fig. 1). The LT50 was also correlated with field winterhardiness and the USDA cold hardiness zone (Fig. 2). LT50s of the commercial cultivars ranged from −20 to −10 °C, and as expected, the hardiest cultivars, such as GV, had the lowest LT50s (Supplemental Table 2). When focusing on the elite genotypes, the percentage of electrolyte leakage at −15 and −20 °C was highly correlated with winterhardiness recorded in Olds and Saskatoon, respectively (Fig. 3). The LT50s estimated for the elite roses was strongly correlated with winterhardiness recorded in Saskatoon (Fig. 3).

Linkage maps. The parental maps for CA60 and 'SITR' were slightly modified from the previous published maps (Rouet et al., 2019) to include all individuals for which electrolyte leakage and winterhardiness data were available. The newly created genetic map for CA60 included 140 individuals and spanned 31 linkage groups with 814 simplex SNP markers across 1863 cM.

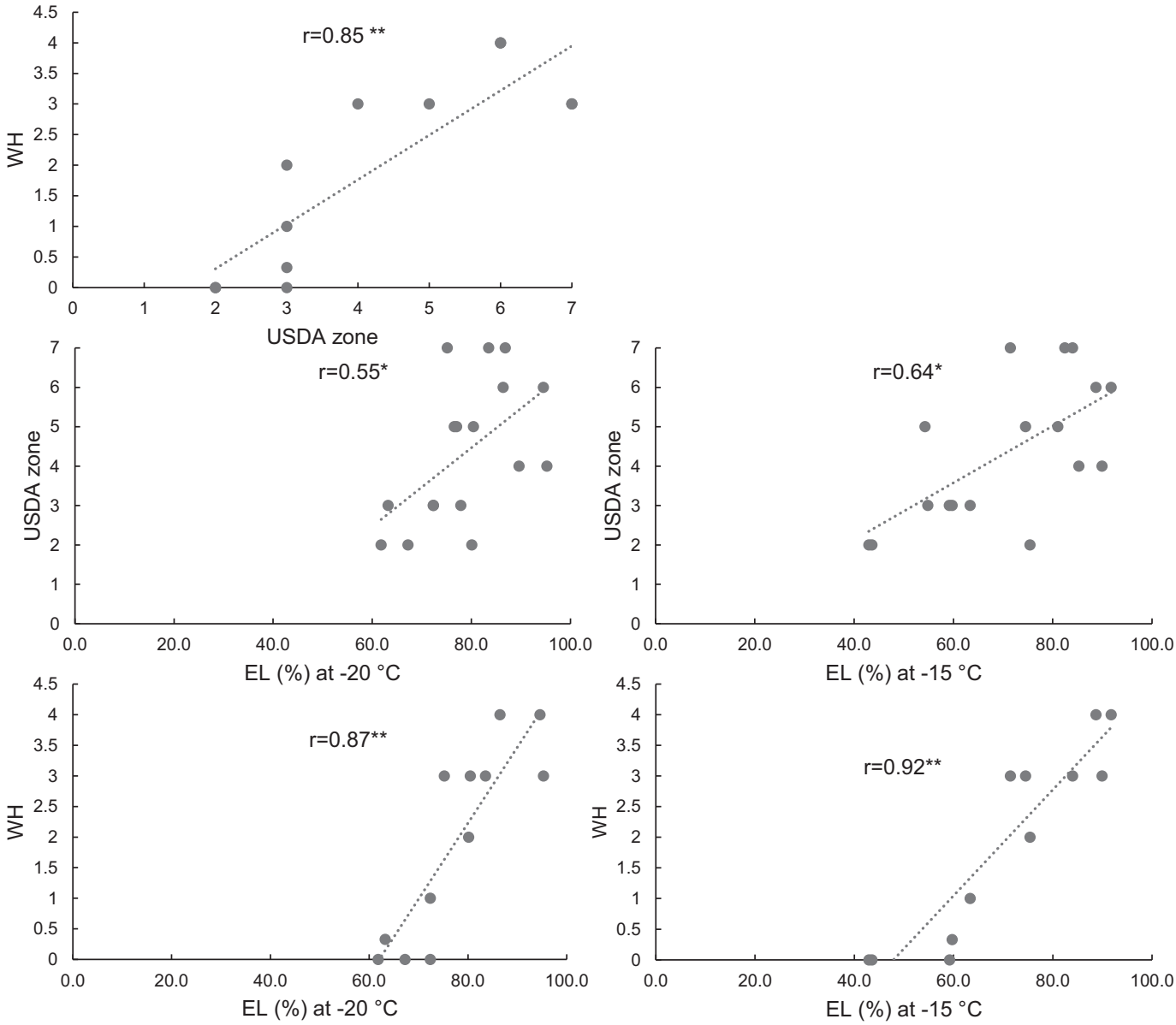

Fig. 1. Correlations between U.S. Department of Agriculture (USDA) cold hardiness zones, winterhardiness [WH (0–5 scale: 0 = no winter damage, 1 = damage on the tips of the canes only, 2 = damage down to the snow line, 3 = damage to the crown with good spring regrowth, 4 = damage to the crown with poor spring regrowth, 5 = dead plant)] at Vineland, ON, Canada in 2018 and electrolyte leakage (EL) measured at different temperatures in artificial freezing experiments for 17 *Rosa* ×*hybrida* commercial cultivars. Correlations were computed using the Pearson method. Only significant correlations are given, with * indicating significant correlation at $P = 0.05$ and ** significant correlation at $P = 0.01$.

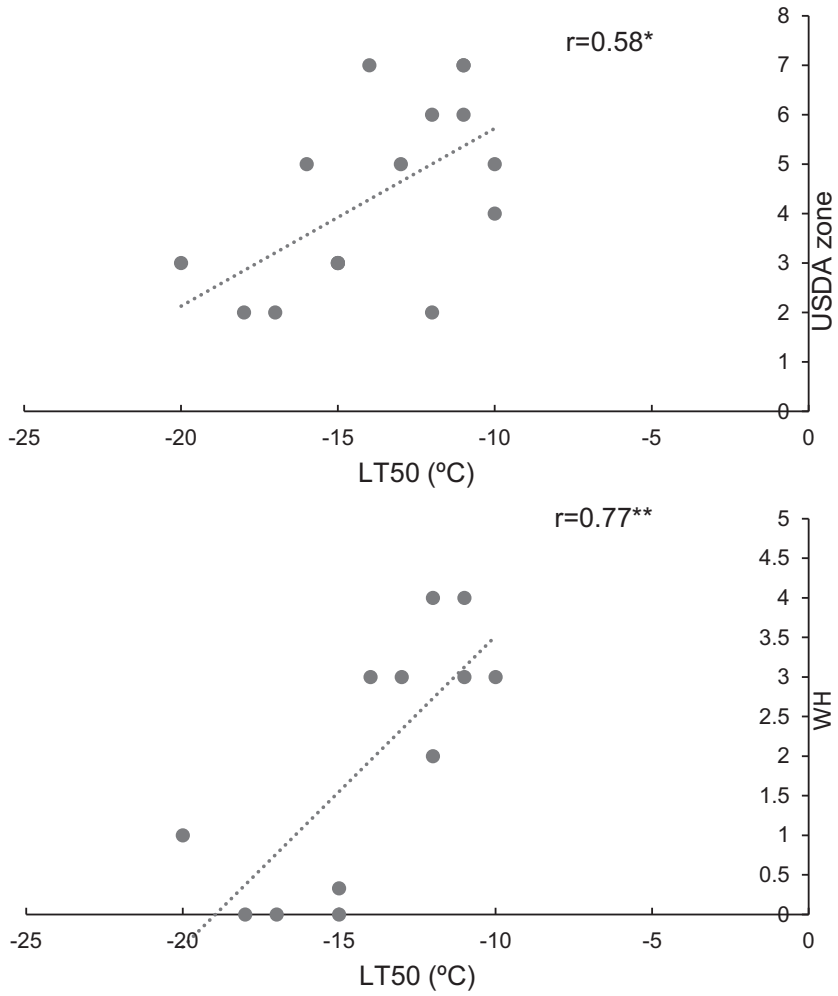

Fig. 2. Correlations between U.S. Department of Agriculture (USDA) cold hardiness zones, winterhardiness [WH (0–5 scale: 0 = no winter damage, 1 = damage on the tips of the canes only, 2 = damage down to the snow line, 3 = damage to the crown with good spring regrowth, 4 = damage to the crown with poor spring regrowth, 5 = dead plant)] at Vineland, ON, Canada in 2018 and the lethal temperature for which 50% of the plants are dead (LT50) estimated using a logit model approach for 17 *Rosa* ×*hybrida* commercial cultivars. Correlations were computed using the Pearson method. Only significant correlations are given, with * indicating significant correlation at $P = 0.05$ and ** significant correlation at $P = 0.01$.

The length of the linkage groups varied from 6 to 150 cM with a mean interval distance between markers of 2.3 cM. The newly created genetic map for 'SITR' included 130 individuals and spanned 29 linkage groups with 660 simplex SNP markers across 1773 cM. The length of linkage groups varied from 8 to 161 cM with a mean interval distance between markers of 2.7 cM. Some homologs were missing, and others were fragmented and were represented by more than one fragment. In addition, rearrangements in marker order were observed in comparison with the reference *R. chinensis* 'Old Blush' homozygous Genome v2.0 (Raymond et al., 2018). The parental maps for 'EDI' and 'GV' were created from newly generated GBS data. A total of 5211 simplex SNP markers that were heterozygous in 'EDI' and homozygous in 'GV' were identified, and 2940 simplex SNPs that were homozygous in 'EDI' and heterozygous in 'GV' were identified. The 'EDI' female map included 97 individuals and spanned 29 linkage groups with 685 simplex SNP markers across 2093 cM. The length of linkage groups varied from 6 cM to 139 cM with a mean interval distance between markers of 3 cM. The 'GV' male map included 97 individuals and spanned 24 linkage groups across 1799 cM with 489 simplex SNP markers and a mean interval distance between markers of 3.7 cM. The length of linkage groups varied from 6 to 149.5 cM.

Expt. 2: QTL mapping of electrolyte leakage

Calibration with parental lines. Electrolyte leakage experiments on the four parental genotypes, conducted to establish the range of freezing temperatures that would be further implemented to screen their segregating progeny, were highly repeatable (Table 2). However, the electrolyte leakage did not increase from −30 to −50 °C in the third replication (data not shown). The data on CA60 and 'GV' in the fourth replication were in the same range as the first and second replications (Supplemental Fig. 1). Therefore, the third replication was removed from the analysis most likely because of a technical issue with the freezer. Only the first two replications were retained for the statistical analysis. The mixed model analysis indicated that the electrolyte leakage and the index of injury were genotype-dependent (Supplemental Table 2). In addition, there were significant differences between the amount of electrolyte leakage and the LT50 of the parental genotypes (Fig. 4, Supplemental Table 3).

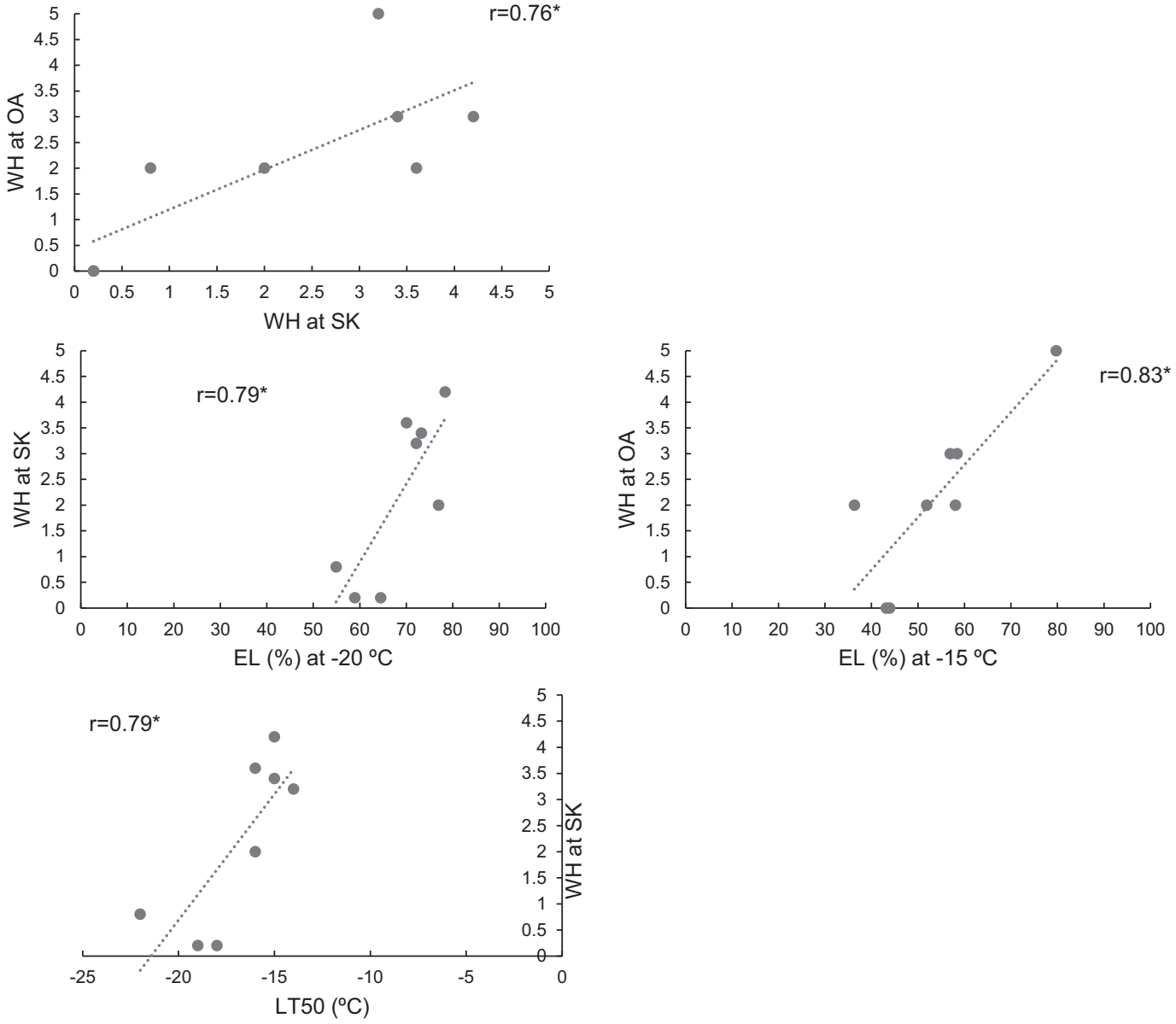

Fig. 3. Correlations between field winterhardiness [WH (0–5 scale: 0 = no winter damage, 1 = damage on the tips of the canes only, 2 = damage down to the snow line, 3 = damage to the crown with good spring regrowth, 4 = damage to the crown with poor spring regrowth, 5 = dead plant)] at Olds, AB, Canada (OA), and Saskatoon, SK, Canada (SK), and electrolyte leakage (EL) measured at different temperatures in artificial freezing experiments for eight elite *Rosa* ×*hybrida* genotypes selected at Vineland, ON, Canada. Correlations between the lethal temperature for which 50% of the plants are dead (LT50) estimated using a logit model approach and field data are also given. Correlations were computed using the Pearson method. Only significant correlations are given, with * indicating significant correlation at $P = 0.05$.

CA60 × 'SITR' population. Electrolyte leakage experiments conducted on 100 F_1 progeny and their two parental genotypes over three temperatures (−10, −15, and −20 °C) were highly repeatable (Table 2), and the BLUPs of electrolyte leakage were obtained from the mixed model analysis (Supplemental Table 4). Although the LT50 could not be calculated in this experiment without the index of injury, the amount of electrolyte leakage for CA60 and 'SITR' at −20 °C (59% and 66%, respectively) were comparable to the values found in the experiment on the parental lines (58% and 71%, respectively). Within the population, as the experimental temperature decreased, the amount of electrolyte leakage increased from 28% (−10 °C) to 54% (−20 °C) (Supplemental Fig. 2). The amount of electrolyte leakage ranged from 41% to 74% at −20 °C, suggesting the existence of large unidirectional transgressive segregation (Table 3). Three QTL associated with electrolyte leakage were identified (Table 4, Supplemental Figs. 3 and 4). A QTL for electrolyte leakage at −10 °C explaining 22% of the phenotypic variance mapped to LG3.H1 at 15 cM in the CA60 female map. A QTL for electrolyte leakage at −20 °C explaining 15% of the phenotypic variance mapped to LG2.H1 at 99 cM in the CA60 female map. A QTL for electrolyte leakage at −20 °C explaining 13% of the phenotypic variance also mapped to LG2.H5 at 15 cM in the 'SITR' male map.

'EDI' × 'GV' population. Electrolyte leakage experiments were conducted on 88 F_1 progeny over a wide range of sub-zero

Table 2. Correlation among three replications (Rep) of electrolyte leakage experiments conducted separately on the *Rosa* ×*hybrida* genotypes CA60, Easy Does It ['EDI' ('HARpageant')], Singin' in the Rain ['SITR' ('MACivy')], and 'George Vancouver' ('GV'), the mapping population CA60 ×'SITR', and the mapping population 'EDI'× 'GV'. Pearson coefficients of correlation are given in the table and significant correlations at $\alpha = 0.01$ are given by *.

Parental lines					
Electrolyte leakage					
	Rep 1	Rep 2	Rep 3		
Rep 1		0.95*	0.94*		
Rep 2			0.95*		
Rep 3					
Index of injury[z]					
	Rep 1	Rep 2	Rep 3		
Rep 1		0.93*	0.88*		
Rep 2			0.88*		
Rep 3					
CA60 × 'SITR' population					
Electrolyte leakage					
	Rep 1	Rep 2	Rep 3	Rep 4	Rep 5
Rep 1		0.77*	0.77*	0.79*	0.73*
Rep 2			0.76*	0.78*	0.72*
Rep 3				0.76*	0.75*
Rep 4					0.80*
Rep 5					
'EDI' × 'GV' population					
Electrolyte leakage					
	Rep 1	Rep 2	Rep 3		
Rep 1		0.72*	0.72*		
Rep 2			0.75*		
Rep 3					
Index of injury					
	Rep 1	Rep 2	Rep 3		
Rep 1		0.70*	0.71*		
Rep 2			0.75*		
Rep 3					

[z]In addition to electrolyte leakage (%), the index of injury (%) was also recorded for the parental lines and the mapping population 'EDI' × 'GV'.

temperatures from −15 to −45 °C with a measurement taken at 4 °C for a control. The experiments were highly repeatable (Table 2), the BLUPs of electrolyte leakage were obtained from the mixed model analysis (Supplemental Table 4), and the LT50s were obtained for each genotype (Supplemental Table 5). Although the parental genotypes 'EDI' and 'GV' were not included in this experiment, inferences on their LT50s could be made based on the experiments conducted on the parental genotypes (Supplemental Table 3). Within the population, the amount of electrolyte leakage increased from 47% (−15 °C) to 78% (−45 °C) as the experimental temperature decreased (Supplemental Fig. 2) without evidence for transgressive segregation (Table 3). Four QTL for electrolyte leakage and LT50 were identified (Table 4, Supplemental Figs. 5 and 6). A QTL for electrolyte leakage at −20 °C explaining 18% of the phenotypic variance mapped to LG6.H1 at position 45 cM in the 'EDI' female map. QTL for electrolyte leakage at −20 °C and for LT50 mapped to the same position on LG7.H1 at 135 cM in the 'GV' male map. The two QTL explained 14% and 16% of the phenotypic variance respectively. A QTL for electrolyte leakage at −35 °C mapped to LG7.H3 at 20 cM in the 'GV' male map, and it explained 22% of the phenotypic variance.

Expt. 3: QTL mapping of field-based winterhardiness

CA60 × 'SITR' population. The CA60 × 'SITR' population was evaluated over 2 years at two locations with very different climates. Winter temperatures in Saskatoon (USDA hardiness zone 3b) were colder than in Elora (USDA hardiness zone 5b). Temperature is Saskatoon reached −40 °C during the colder months of the first winter with minimal snow cover. In addition, sub-zero temperatures were recorded for up to 40 consecutive days in Saskatoon between February and Mar. 2019, while sub-zero temperatures were recorded for less than 10 consecutive days in Elora. Environmental conditions also varied at the same location across years, the number of consecutive days with sub-zero temperatures was reduced in Sask 2020 in comparison with Sask 2019, but the number of freeze-thaw cycles increased (Supplemental Fig. 7). Although the winter temperatures were consistent in Elora across years, severe disease pressure occurred in Fall 2019.

Winter damage, which was the first aspect of field winterhardiness, varied across environments (Fig. 5A–D). As expected, cold-susceptible genotypes suffered higher damage than the hardy control and parental genotypes (Fig. 5E–H). The data from Sask 2020 were highly skewed toward extreme winter damage and not informative, as 90% of the population exhibited more than 95% winter damage (Fig. 5D); therefore, Sask 2020 was dropped from the rest of the winter damage analysis. The GE interaction was significant for the three remaining environments with a high $\frac{V_{ge}}{V_g}$ ratio ($\frac{V_{ge}}{V_g} = 1.33$), where V_{ge} is the variance associated with the GE interaction; therefore, the BLUPs of winter damage were obtained separately for each of these environments (Supplemental Table 6). GGE-biplots were generated using the BLUPs of winter damage to further visualize the relationships between the environments and characterize the nature of GE interaction. The two principal components PC1 and PC2 of the GGE-biplot explained 71.51% and 20.8% of the GGE variation, respectively, meaning that the two sources of variation G plus GE explained 92.31% of the total phenotypic variance (Fig. 6). The angle between the environment vectors associated with Elora 2019 and Sask 2019 was acute, meaning that the environments were positively correlated without crossovers GE patterns; however, the vector associated with Elora 2019 was longer than that of Sask 2019. Therefore, Elora 2019 was more discriminative than Sask 2019, and the nature of the GE interaction was mainly a change in magnitude due to the severity of the climatic conditions in Saskatoon. Furthermore, Elora 2019 and Elora 2020 were distant on the GGE-biplot, meaning that the two environments discriminated the genotypes differently based on winter damage with minor patterns of GE crossovers (Fig. 6). These observations were supported by the Pearson's correlations (Table 5). The heritability of winter damage varied by location and year; it was high in Elora 2019, but it was low in Sask 2019 and Elora 2020, ranging from 0.13 to 0.83 (Table 6). Noticeably, pest-induced defoliation that occurred in Elora 2019 was positively and highly correlated with winter damage in Elora 2020 (Table 5). Overall, Elora 2019 was the least severe environment, with a population mean of 51% winter damage, whereas Sask 2019 was the most severe environment

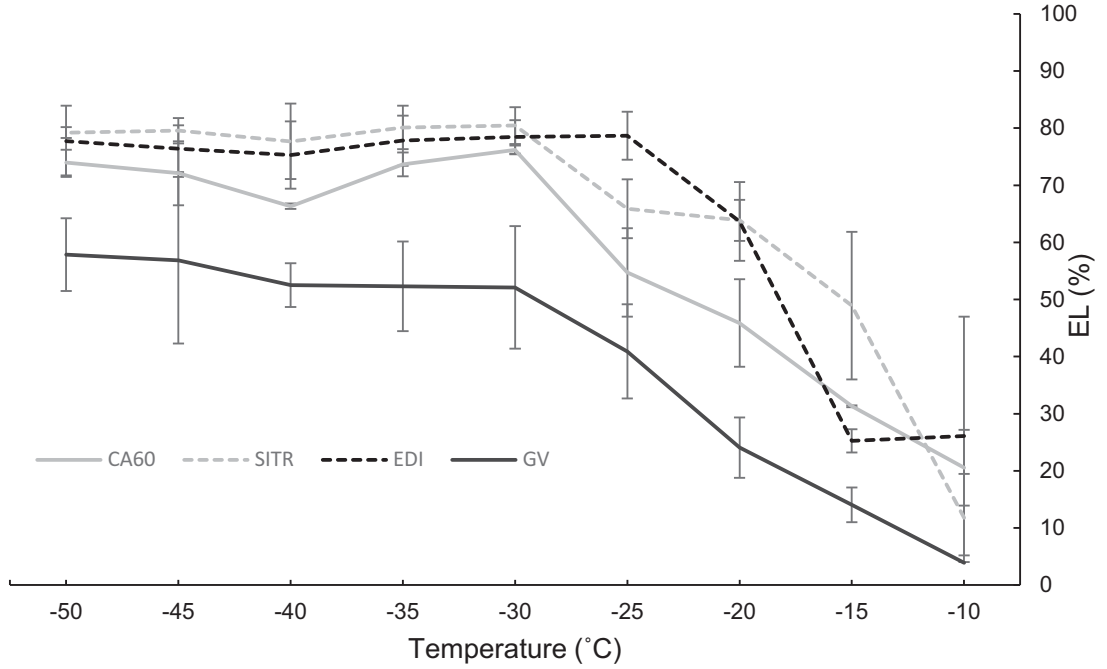

Fig. 4. Response of four *Rosa* ×*hybrida* genotypes, CA60, Singin' in the Rain ['SITR' ('MACivy')], Easy Does It ['EDI' ('HARpageant')], and 'George Vancouver' ('GV'), to freezing treatment from −10 to −50 °C. Sensitivity to freezing is displayed as the BLUE estimates of the index of injury (I) [electrolyte leakage (EL) corrected for leakage not due to freezing damage (i.e., control)], estimated from two replications of EL assays.

with a population mean of 81% winter damage (Table 3). There was evidence for transgressive segregation beyond both parental values (Table 3), with 4% of individuals that were as hardy as the hardiest parent CA60 and 30% that were as sensitive or more sensitive than the tender parent 'SITR' in Elora 2019.

The second aspect of field winterhardiness in this study was spring regrowth. Regrowth in the population and the control and parental genotypes did not vary across environments as winter damage did (Fig. 7A and B). Although 'SITR' and CA60 did not differ in Elora 2019, 'SITR' had inferior potential for regrowth in the other environments compared with CA60 (Fig. 7B). The mixed model analysis of the four environments indicated significant GE interaction and high $\frac{Vge}{Vg}$ ratio [$\frac{Vge}{Vg} = 3.09$ (Supplemental Table 7)]. The BLUPs for regrowth were obtained separately for each environment (Supplemental Table 7) and visualized with a GGE-biplot (Fig. 6). The two principal components PC1 and PC2 explained 44.41% and 28.9% of the GGE variation, respectively, meaning that G and GE explained 73.31% of the total phenotypic variance (Fig. 6). The right angle between the vectors associated with Saskatoon and the vectors associated with Elora indicate that Saskatoon and Elora environments were not correlated for regrowth. Moreover, the angles between the vectors associated with Sask 2019 and Sask 2020 and between Elora 2019 and Elora 2020 were acute, indicating that regrowth was positively correlated at each location across years. This was corroborated by the Pearson's correlations (Table 5). Elora 2019 and Sask 2019 had the longest vectors, meaning that they were more capable of discriminating among genotypes than Elora 2020 and Sask 2020 (Fig. 6). The heritability of regrowth was moderate to high, with the highest estimate obtained for Elora 2019 (Table 6). Overall, regrowth was higher in 2019 than in 2020 at both locations, and there was evidence for transgressive segregation beyond both parents (Table 3). Winter damage and regrowth were not correlated in most environments, which suggested that regrowth and winter damage were inherited separately. However, regrowth and winter damage were highly correlated in Elora 2020 (Table 5). Noticeably, pest-induced defoliation recorded in Elora 2019 was highly correlated with regrowth in Elora 2020 (Table 5).

QTL analysis for winter damage and regrowth was conducted separately for each environment because of the existence of significant GE interaction (Table 4, Supplemental Figs. 3 and 4). A QTL for winter damage in Elora 2019 mapped to LG2.H1 at 55 cM in the CA60 female map. This QTL alone explained 16% of the total phenotypic variance. A major QTL for winter damage in Elora 2019 mapped to LG2.H5 at 17 cM in the 'SITR' male map. A minor QTL for winter damage in Elora 2019 mapped to a fragment of LG5.H1 at 10 cM in the 'SITR' male map. The two-QTL model explained 30% of the phenotypic variance. A QTL for winter damage in Sask 2019 mapped to LG6.H1 at 20 cM in the 'SITR' male map and it explained 17% of the phenotypic variance. A QTL for winter damage in Elora 2020 mapped to LG1.H3 at 10 cM in the CA60 female map, explaining 24% of the phenotypic variation. No QTL for winter damage in Sask 2020 were detected. In addition, a QTL for regrowth in Elora 2019 mapped to LG7.H1 at 40 cM in the CA60 female map; it explained 14% of the phenotypic variance. A QTL for regrowth in Elora 2020 mapped to LG1.H3 at 20 cM in CA60—10 cM away from the QTL for winter damage in the same environment—and explained 37% of the phenotypic variance. A QTL for regrowth in Elora 2020 mapped to LG6.H4 at 60 cM in the 'SITR' male map, and it explained 15% of the phenotypic variance. A QTL for regrowth in Sask 2019 mapped to LG6.H2 at 20 cM in the CA60 female map, and it explained 18% of the phenotypic variance. A QTL for regrowth in Sask 2019 mapped to LG6.H1 at 20 cM in the 'SITR' male map, and it explained 18% of the phenotypic variance. No QTL for regrowth in Sask 2020 were detected. A QTL for defoliation that occurred in

Table 3. Evidence for transgressive segregation for electrolyte leakage (EL), field winter damage (WD), and field spring regrowth (RG) in the *Rosa* ×*hybrida* mapping populations CA60 × Singin' in the Rain ['SITR' ('MACivy')] and Easy Does It™ ['EDI' ('HARpageant')] × 'George Vancouver' ('GV') and their parental lines, which differ in their hardiness level.

EL (%)[z]	EL (%) at −20 °C				EL (%) at −25 °C
	Parental genotypes				
CA60	58				65
'SITR'	71				72
'EDI'	71				83
'GV'	43				55
	CA60 × 'SITR' population				
Mean[y]	54				
Maximum	74				
Minimum	41				
	'EDI' × 'GV' population				
Mean					71
Maximum					78
Minimum					62
WD (%)[x]	Elora 2019	Elora 2020	Sask 2019	Sask 2020	Elora 2020
	Parental genotypes				
CA60	33	64	83		14
'SITR'	55	94	83		91
'EDI'	71	94	95		85
'GV'	19	55	8		34
	CA60 × 'SITR' population				
Mean	51	74	81		
Maximum	71	97	9		
Minimum	24	21	64		
	'EDI' × 'GV' population				
Mean					58
Maximum					92
Minimum					12
RG (%)[w]	Elora 2019	Elora 2020	Sask 2019	Sask 2020	Elora 2020[v]
	Parental genotypes				
CA60	87	103	126	76	96
'SITR'	90	67	81	69	65
'EDI'	81	71			70
'GV'	47	61	110	80	96
	CA60 × 'SITR' population				
Mean	94	79	103	77	
Maximum	140	102	149	92	
Minimum	60	41	73	56	
	'EDI' × 'GV' population				
Mean					89
Maximum					148
Minimum					53

[z]EL was recorded at −10, −15, −20, −25, −30, −35, and −40 °C for the 'EDI' × 'GV' population, and at −10, −15, and −20 °C for the CA60 × 'SITR' population. EL was recorded at 4 (i.e., control), −10, −15, −20, −25, −30, −35, −40, −45, and −50 °C for the parental lines. The temperature for which the highest segregation was observed among the population is reported in this table.

[y]The population mean, minimum, and maximum values are reported.

[x]WD was a measurement of cane dieback using the following formula: $WD\ (\%) = 100 \times \frac{ld}{lt}$, with WD being the percentage of winter damage, ld the length of dieback, and lt the length of the whole cane.

[w]RG was estimated with the following formula: $RG\ (\%) = 100 \times \frac{ln}{lt}$, with RG being the percentage of regrowth, ln the length of the new shoot, and lt the initial length of the whole cane. For both WD and RG, three stems per plant were measured and the average value for each plant was used as the final rating.

[v]Both WD and RG were measured in four environments consisting of two locations (Elora, ON, Canada; Saskatoon, SK, Canada) and 2 years (2019–20) (Elora 2019, Elora 2020, Sask 2019, and Sask 2020). The CA60 × 'SITR' trial was conducted over Elora 2019, Elora 2020, Sask 2019, and Sask 2020, and the 'EDI' × 'GV' trial was conducted in Elora 2020 only. The four parental lines were planted within each trial.

Table 4. Quantitative trait loci (QTL) associated with electrolyte leakage (EL), field winter damage (WD), field spring regrowth (RG), and defoliation in two *Rosa* ×*hybrida* mapping populations CA60 × Singin' in the Rain™ ['SITR' ('MACivy')] and Easy Does It™ ['EDI' ('HARpageant')] × 'George Vancouver' ('GV').

								Genotype[u]	
QTL label[z]	Trait[y]	Map[x]	LG[w]	LOD	Marker peak	Flanking markers	PVE (%)[v]	AB	AA
qEL10.CA60xSITR-ch3.2019	EL (%) at −10 °C	CA60	LG3.H1	5.59	29705230	16726330 … 38175338	22	29.55	26.85
q1EL20.CA60xSITR-ch2.2019	EL (%) at −20 °C	CA60	LG2.H1	2.99	86652613	81996645 … 86652613	15	52.29	56.75
q2EL20.CA60xSITR-ch2.2019		SITR	LG2.H5	2.37	60933255	67472600 … 81894926	13	52.42	56.36
qEL20.EDIxGV-ch6.2020		EDI	LG6.H1	3.68	38291929	32920513 … 38292014	18	60.25	62.84
qEL20.EDIxGV-ch7.2020		GV	LG7.H1	2.77	57129108	50501062 … 67941547	14	60.21	62.61
qEL35.EDIxGV-ch7.2020	EL (%) at −35 °C	GV	LG7H3	4.8	176793	176793 … 1997550	22	78.57	80.41
qLT50.EDIxGV-ch7.2020	LT50 (°C)	GV	LG7H1	3.08	57129108	50501062 … 62247052	16	−21.08	−18.7
q1WDElora.CA60xSITR-ch2.2019	WD Elora 2019	CA60	LG2.H1	3.20	65756692	69386276 … 81071479	16	49.24	56.63
q2WDElora.CA60xSITR-ch2.2019		SITR	LG2.H5	4.93	81894926	71623330 … 81894926	21	48.59	56.45
qWDElora.CA60xSITR-ch5.2019			LG5.H1	3.11	65876381	35540595 … 75948827	11	54.74	48.86
qWDElora.CA60xSITR-ch1.2020	WD Elora 2020	CA60	LG1.H3	5.61	67169791	66170115 … 67492819	24	66.40	83.11
qWDElora.EDIxGV-ch6.2020		EDI	LG6.H2	3.30	68093598	67121912 … 69256534	15	50.27	64.72
qWDElora.EDIxGV-ch5.2020		GV	LG5.H2	2.55	28914028	25970959 … 53663853	14	51.13	64.84
qWDSask.CA60xSITR-ch6.2019	WD Sask 2019	SITR	LG6.H1	3.26	54366335	40154937 … 62419734	17	82.72	77.64
qRGElora.CA60xSITR-ch7.2019	RG Elora 2019	CA60	LG7.H1	2.88	4530588	23986267 … 37107077	14	97.11	88.43
qRGElora.CA60xSITR-ch1.2020	RG Elora 2020	CA60	LG1.H3	10.18	66233855	66170116 … 66233855	37	85.54	72.02
qRGElora.CA60xSITR-ch6.2020		SITR	LG6.H4	3.06	66596604	55947087 … 62762841	15	73.98	82.51
qRGElora.EDIxGV-ch5.2020		EDI	LG5.H2	3.05	10621719	4837677 … 17237029	14	97.48	82.05
qRGElora.EDIxGV-ch2.2020		GV	LG2.H2	3.03	68182818	59928853 … 79522994	14	83.18	99.55
q1RGSask.CA60xSITR-ch6.2019	RG Sask 2019	CA60	LG6.H2	4.19	47563687	27091872 … 63202691	16	108.43	97.42
q2RGSask.CA60xSITR-ch6.2019		SITR	LG6.H1	4.03	54366335	53244936 … 55947116	18	97.10	108.74
qDEF.CA60xSITR-ch1.2020	Defoliation	CA60	LG1.H3	10.17	67169791	66170116 … 66233855	36	2.551	3.681

[z]The QTL analysis was conducted using multiple QTL mapping (MQM) with the software R Studio (R Foundation for Statistical Computing, Vienna, Austria). QTL were labeled according to the Genome Database for Rosaceae (GDR) naming protocol.

[y]Field data were collected from four environments consisting of two locations (Elora, ON, Canada; Saskatoon, SK, Canada) and 2 years (2019–20) (Elora 2019, Elora 2020, Sask 2019, and Sask 2020). WD was a measurement of cane dieback using the following formula: $WD\ (\%) = 100 \times \frac{ld}{lt}$, with WD being the percentage of winter damage, ld the length of dieback, and lt the length of the whole cane. RG was estimated with the following formula: $RG\ (\%) = 100 \times \frac{ln}{lt}$, with RG being the percentage of regrowth, ln the length of the new shoot, and lt the initial length of the whole cane. For both WD and RG, three stems per plant were measured and the average value for each plant was used as the final rating. EL was recorded at −10, −15, −20, −25, −30, −35, and −40 °C for the 'EDI' × 'GV' population, and at −10, −15, and −20 °C for the CA60 × 'SITR' population.
Defoliation was recorded in Elora 2019 (0–4 scale: 0 = no defoliation and intact leaves, 1 = minor damages to the leaves mainly caused by caterpillars, 2 = minor defoliation with leaves left all over the rose bush, 3 = leaves left only on the tips of the stems, 4 = no leaves left, severe defoliation).

[x]Mapping was conducted separately for each parental lines CA60, 'EDI', 'SITR', and 'GV'. All QTL for which the logarithm of odds (LOD) score was above the LOD threshold were reported. The markers were named based on their relative positions in the reference genome *Rosa chinensis* (Raymond et al., 2018).

[w]LG Linkage group and homologous chromosome H.

[v]Percentage of variance explained.

[u]Phenotypic means are given for each genotypic group (AA homozygous allele and AB heterozygous allele) at a single putative QTL position.

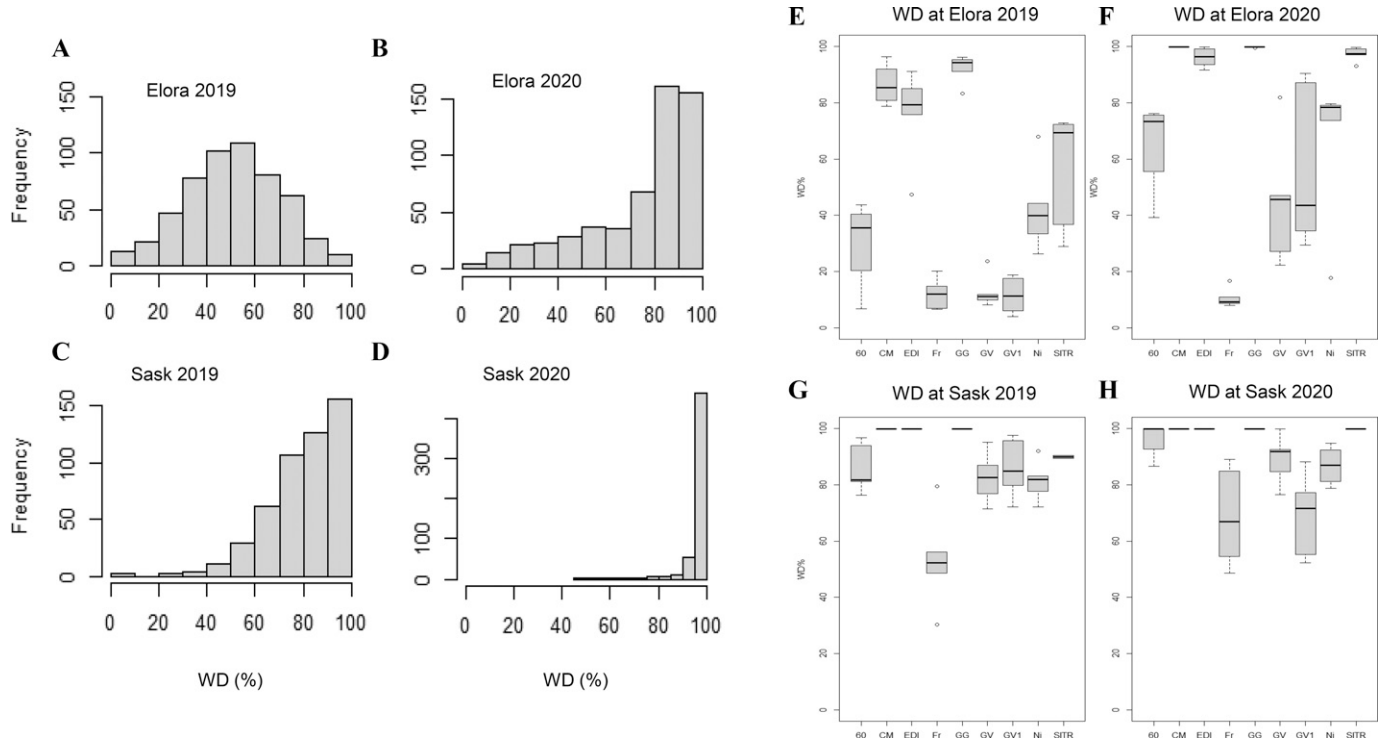

Fig. 5. Distribution of field winter damage (WD) in the *Rosa ×hybrida* mapping population CA60 × Singin' in the Rain [SITR ('MACivy')] in four environments: Elora, ON, Canada in (**A**) 2019 (Elora 2019) and (**B**) 2020 (Elora 2020), Saskatoon, SK, Canada in (**C**) 2019 (Sask 2019) and (**D**) 2020 (Sask 2020), and distribution of WD among the parental and control genotypes used in (**E**) Elora 2019, (**F**) Elora 2020, (**G**) Sask 2019, and (**H**) Sask 2020. WD was a measurement of cane dieback in the field using the following formula: $\text{WD } (\%) = 100 \times \frac{\text{ld}}{\text{lt}}$, with WD being the percentage of winter damage, ld the length of dieback, and lt the length of the whole cane. Data on three canes per plant were collected and averaged. The parental and control genotypes can be divided into cold-hardy ['Frontenac' (Fr), 'George Vancouver' (GV), GV grown on its own roots (GV1), 'Nicolas' (Ni), and CA60 (60)] and non–cold-hardy genotypes [Gentle Giant (GG), Caroline de Monaco® (CM), Easy Does It (EDI), and SITR] relative to their U.S. Department of Agriculture (USDA) cold hardiness zones.

Elora in 2019 mapped to LG1.H3 at 15 cM in the CA60 female map and explained 36% of the phenotypic variance.

'EDI' × 'GV' POPULATION. Winter damage and regrowth were recorded in one environment (Elora 2020). Winter damage was distributed around a mean of 58% with minimum damage of 12% and maximum damage of 92%, and regrowth was distributed around a mean of 89% with minimum regrowth of 53% and maximum regrowth of 148% (Fig. 8, Table 3). The control genotypes CA60 and 'SITR' and the parental lines 'EDI' and 'GV' differed, but their respective ratings were similar to the CA60 × 'SITR' multisite field trial (Table 3). The female parent 'EDI' exhibited substantial winter damage (85%), close to total dieback to the ground, whereas the male parent 'GV' presented minimal winter damage [34% (Fig. 8)]. Regrowth of 'GV' appeared greater than 'EDI' [96% and 70%, respectively (Table 3)]. There was evidence for transgressive segregation beyond both parents for both winter damage and regrowth (Table 3), with 7% of individuals that were as hardy as the hardiest parent 'GV' and 11% that were as sensitive or more sensitive than the tender parent 'EDI'. The genotypic variance was significant for both winter damage and regrowth (Supplemental Tables 6 and 7). Both winter damage and regrowth were heritable (Table 6), but regrowth and winter damage were not correlated for the 'EDI' × 'GV' population (Table 5). QTL for winter damage and regrowth mapped to different linkage groups (LGs) of the rose genome (Table 4, Supplemental Figs. 5 and 6). A QTL for winter damage in Elora 2020 mapped to LG6.H2 at 10 cM in the 'EDI' female map; this QTL explained 15% of the variability observed. A QTL for winter damage in Elora 2020 also mapped to LG5.H2 at 65 cM in 'GV'. This QTL explained 14% of the phenotypic variance. In addition, a QTL for regrowth mapped to LG2.H2 at 30 cM in the 'GV' male map and explained 14% of the observed phenotypic variation. A QTL for regrowth mapped to LG5.H2 at 50 cM in the 'EDI' female map and explained 14% of the phenotypic variance.

Relationship between electrolyte leakage and field winterhardiness

Electrolyte leakage measured at −20 °C under artificial conditions was positively but poorly correlated with winter damage in all environments for the CA60 × 'SITR' population, with the highest correlation being in the environment Elora 2019 and the weakest being in Elora 2020 (Table 7). Electrolyte leakage measured at −25 °C under artificial conditions was poorly correlated with winter damage for the 'EDI' × 'GV' population, and the LT50 did not correlate with winter damage (Table 7). Different levels of freezing tolerance under artificial conditions were identified for each individual in both mapping populations based on the distribution of electrolyte leakage data; individuals were grouped into three categories of electrolyte leakage according to their affiliation to either the first quartile of the distribution, the second and third quartiles, or the fourth quartile, and their level of freezing tolerance was compared with their level of field winterhardiness. For both populations, although the individuals from the first quartile had the least electrolyte leakage, they did not consistently show the least winter damage in the field.

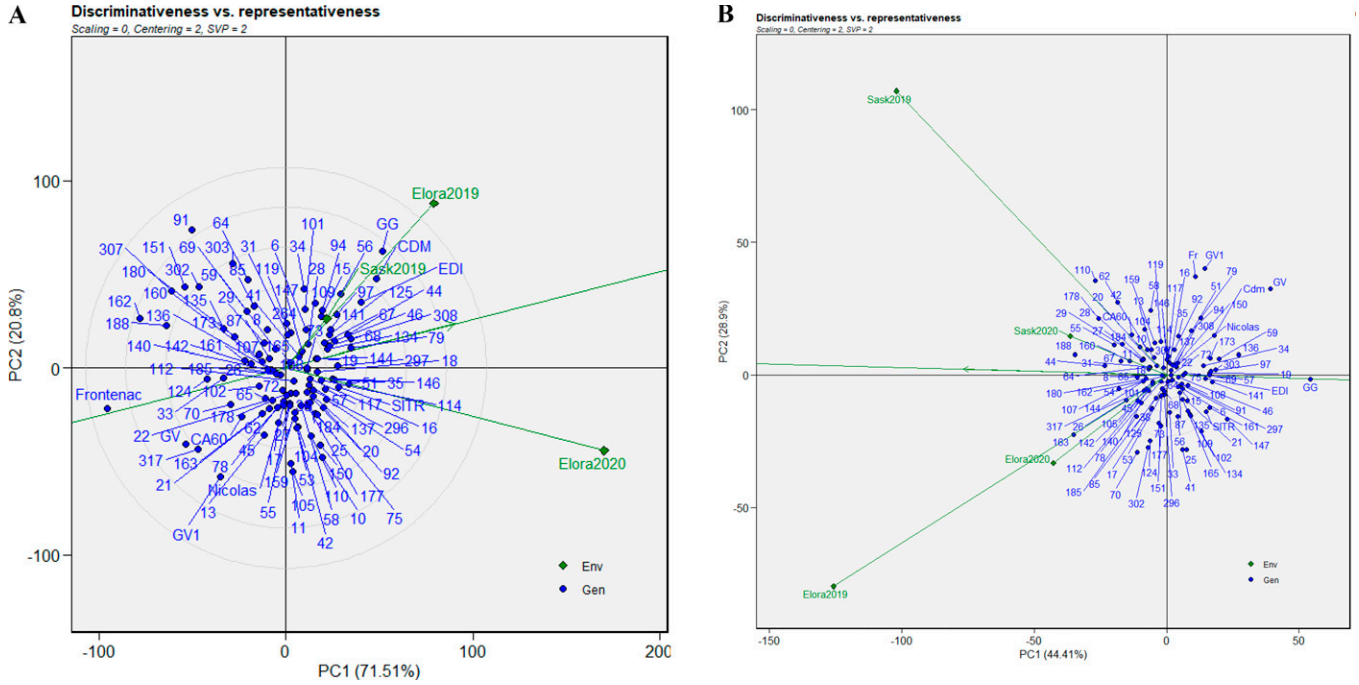

Fig. 6. Environment-metric preserving biplot representing genotype plus genotype × environment interaction (GGE) and generated from best linear unbiased predictors (BLUPs) of (**A**) field winter damage (WD) and (**B**) regrowth (RG) in the *Rosa* ×*hybrida* mapping population CA60 × Singin' in the Rain [SITR ('MACivy')]. The length of the environment vectors provides information on the ability of an environment to discriminate among genotypes, whereas the distance between environment markers and the angles between the environment vectors are associated with the correlation between environments. The GGE-biplot model uses the principle of singular value decomposition (SVD) to decompose genotype (G) and genotype × environment (GE) effects into two components represented as principal components (PC1 and PC2) on the graph axis. WD is represented over three environments (Env): Elora, ON, Canada in 2019 (Elora 2019) and 2020 (Elora 2020), and Saskatoon, SK, Canada in 2019 (Sask 2019). RG is represented over four environments: Elora 2019, Elora 2020, Sask 2019, and Saskatoon in 2020 (Sask 2020). WD was a measurement of cane dieback in the field using the following formula: $\text{WD}\ (\%) = 100 \times \frac{\text{ld}}{\text{lt}}$, with WD being the percentage of winter damage, ld the length of dieback, and lt the length of the whole cane. RG was estimated with the following formula: $\text{RG}\ (\%) = 100 \times \frac{\text{ln}}{\text{lt}}$, with RG being the percentage of regrowth, ln the length of the new shoot, and lt the initial length of the whole cane. For both WD and RG, data on three canes per plant were collected and averaged.

Likewise, although the individuals from the fourth quartile had the most electrolyte leakage, they did not consistently show the most winter damage in the field. Consequently, electrolyte leakage did not align with field winterhardiness (Supplemental Fig. 8).

Discussion

Electrolyte leakage appeared as a good proxy for field winterhardiness in a small panel of commercial cultivars; however, it did not align with field winter damage in the breeding material.

Table 5. Correlation between best linear unbiased prediction estimates (BLUPs) of winter damage (WD) in three environments (Elora 2019, Elora 2020, and Sask 2019), defoliation, and BLUPs of regrowth (RG) for four environments: Elora, ON, Canada in 2019 (Elora 2019) and 2020 (Elora 2020), and Saskatoon, SK, Canada in 2019 (Sask 2019) and 2020 (Sask 2020) for the *Rosa* ×*hybrida* mapping population CA60 × Singin' in the Rain™ ['SITR' ('MACivy')], and between BLUPs of WD and RG for the *Rosa* ×*hybrida* mapping population Easy Does It™ ['EDI' ('HARpageant')] × 'George Vancouver' ('GV'). Significant correlations are given by *, **, and ***, indicating significant correlation at $P = 0.05$, $P = 0.01$, and $P = 0.001$, respectively.

	WD[z] Elora 2019	WD Elora 2020	WD Sask 2019	Defoliation[y] Elora 2019	RG[x] Elora 2019	RG Elora 2020	RG Sask 2019	RG Sask 2020
1. CA60 × 'SITR' population								
WD Elora 2019		0.41***	0.28***	0.15				
WD Elora 2020			0.15	0.65***				
WD Sask 2019				0.06				
RG Elora 2019	−0.06	0.09	0.04	0.13		0.16	0.15	0.07
RG Elora 2020	−0.03	−0.44***	0.06	−0.56***			0.04	0.02
RG Sask 2019	−0.19	0.04	−0.25*	0.02				0.29**
RG Sask 2020	−0.15	0	−0.18	−0.11				
2. 'EDI' × 'GV' population								
RG Elora 2020		−0.18						

[z]WD was a measurement of cane dieback using the following formula: $\text{WD}\ (\%) = 100 \times \frac{\text{ld}}{\text{lt}}$, with WD being the percentage of winter damage, ld the length of dieback, and lt the length of the whole cane.

[y]Defoliation was recorded in Elora 2019 (0–4 scale: 0 = no defoliation and intact leaves, 1 = minor damage to the leaves mainly caused by caterpillars, 2 = minor defoliation with leaves left all over the rose bush, 3 = leaves left only on the tips of the stems, 4 = no leaves left, severe defoliation).

[x]RG was estimated with the following formula: $\text{RG}\ (\%) = 100 \times \frac{\text{ln}}{\text{lt}}$, with RG being the percentage of regrowth, ln the length of the new shoot, and lt the initial length of the whole cane. For both WD and RG, three stems per plant were measured and the average value for each plant was used as the final rating.

Table 6. Heritability and variance estimates for field winter damage and regrowth for the *Rosa* ×*hybrida* mapping populations CA60 × Singin' in the Rain™ ['SITR' ('MACivy')] and Easy Does It™ ['EDI' ('HARpageant')] × 'George Vancouver' ('GV').

Population	Trait[z]	Environment[y]	Method[x]	Broad sense heritability[w]	Estimates[v]
CA60 × 'SITR' population	Winter damage	Elora 2019	LMM Gaussian	0.83	Vg = 158.09 Vresidual = 160.73 r = 5
		Elora 2020	GLMM, dist = Beta link = logit	0.29	Vg = 1.0654 r = 5 Φ = 9.9512
		Sask 2019	GLMM, dist = Beta link = logit	0.13	Vg = 0.3156 r = 5 Φ = 7.5348
'EDI' × 'GV' population	Winter damage	Elora 2020	LMM Approx. Gaussian	0.81	Vg = 0.04228 Vresidual = 0.03022 r = 3
CA60 × 'SITR' population	Regrowth	Elora 2019	GLMM dist = lognormal link = identity	0.82	Vg = 0.04041 Vresidual = 0.04457 r = 5
		Elora 2020	GLMM dist = lognormal link = identity	0.77	Vg = 0.03012 Vresidual = 0.04377 r = 5
		Sask 2019	GLMM dist = lognormal link = identity	0.59	Vg = 0.03274 Vresidual = 0.1129 r = 5
		Sask 2020	GLMM dist = lognormal link = identity	0.41	Vg = 0.02542 Vresidual = 0.1435 r = 4
'EDI' × 'GV' population	Regrowth	Elora 2020	GLMM dist = lognormal link = identity	0.53	Vg = 0.05231 Vresidual = 0.14 r = 3

[z]Winter damage (WD) was a measurement of cane dieback using the following formula: $\mathrm{WD}\ (\%) = 100 \times \frac{\mathrm{ld}}{\mathrm{lt}}$, with WD being the percentage of winter damage, ld the length of dieback, and lt the length of the whole cane. Regrowth (RG) was estimated with the following formula: $\mathrm{RG}\ (\%) = 100 \times \frac{\mathrm{ln}}{\mathrm{lt}}$, with RG being the percentage of regrowth, ln the length of the new shoot, and lt the initial length of the whole cane. For both WD and RG, three stems per plant were measured and the average value for each plant was used as the final rating.
[y]Field data were collected from four environments consisting of two locations (Elora, ON, Canada, and Saskatoon, SK, Canada) and 2 years (2019–20) (Elora 2019, Elora 2020, Sask 2019, and Sask 2020).
[x]Heritability of winter damage and regrowth in CA60 × 'SITR' population was estimated for single environments. Data were fitted either a linear mixed model (LMM) with a Gaussian distribution or a general linear mixed model (GLMM) with a beta distribution and logit link function or lognormal distribution and identity link function.
[w]Broad sense heritability used the following equation: $H^2 = \frac{\mathrm{Vg}}{\mathrm{Vg} + \left(\frac{\mathrm{Vr}}{\mathrm{r}}\right)}$, where H^2 was the broad sense heritability, whenever the data could be approximated to a normal distribution.
[v]V_g corresponds to the genetic variance, Vresidual corresponds to the residual variance, and Φ is the scale parameter, they were retrieved from the mixed linear model; r corresponds to the number of blocks in the field trial.

Field winter damage was recorded in two locations—Elora and Saskatoon—over 2 years, but the climatic conditions in Saskatoon during the second year were too extreme to provide meaningful information. QTL were detected for electrolyte leakage, winter damage, and spring regrowth, and no stable QTL were detected for winter damage and spring regrowth across environments.

Relationship between electrolyte leakage and field winter damage

Electrolyte leakage measured under artificial conditions at −15 and −20 °C, and the LT50 were strong indicators of field winterhardiness in a panel of 28 phenotypically distinct commercial cultivars and elite roses (Figs. 1–3). These results were supported by the literature (Ouyang et al., 2019). Ouyang et al. (2019) investigated the usefulness of the electrolyte leakage method in 17 rose cultivars, which were naturally acclimated in the field. The authors demonstrated that the genotypes with the highest and lowest levels of cold hardiness relative to their USDA zone could be identified using electrolyte leakage. Our results suggested that the implementation of electrolyte leakage assays for screening winterhardiness in a timely manner in roses could be a strong asset for a rose breeding program.

However, although electrolyte leakage was a strong indicator of field winterhardiness in cultivars, it did not align with field winter damage for the two mapping populations (Supplemental Fig. 7), as supported by the poor correlation between electrolyte leakage and winter damage in the mapping populations [$r = 0.35$ (Table 7)]. Perhaps, there were larger differences in cold hardiness among the rose cultivars that were specifically chosen for their extreme responses to cold stress than the breeding populations that displayed intermediate phenotypes. These results suggested that electrolyte leakage assays present limited utility for application on breeding material to develop winter-hardy roses

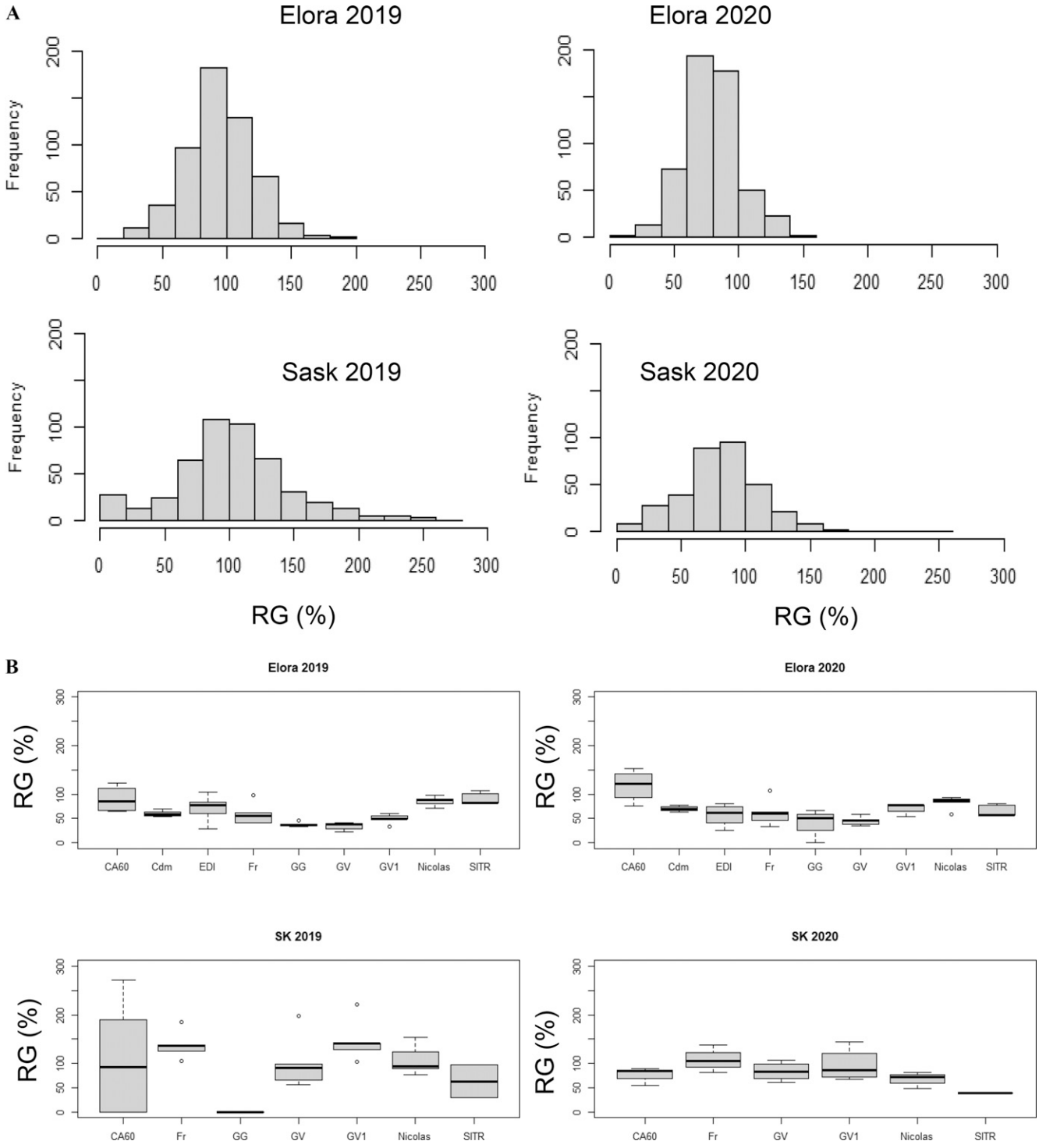

Fig. 7. Distribution of field regrowth (RG) in four environments: Elora, ON, Canada in 2019 (Elora 2019) and 2020 (Elora 2020), and Saskatoon, SK, Canada in 2019 (Sask 2019) and 2020 (Sask 2020) in (**A**) the *Rosa* ×*hybrida* mapping population CA60 × Singin' in the Rain [SITR ('MACivy')] and (**B**) among *Rosa* ×*hybrida* genotypes CA60, Caroline de Monaco [Cdm ('MEIpierar')], Easy Does It™ [EDI ('HARpageant')], 'Frontenac' (Fr), Gentle Giant™ [GG ('WEKrigoyelo')], 'George Vancouver' (GV), GV grown on its own roots (GV1), 'Nicolas' (Ni), and SITR. RG was estimated with the following formula: $\mathrm{RG}\ (\%) = 100 \times \frac{\ln}{\mathrm{lt}}$, with RG being the percentage of regrowth, ln the length of the new shoot, and lt the initial length of the whole cane.

adapted to Elora and Saskatoon. Gusta et al. (1997) studied winterhardiness in winter wheat and suggested that the nature of the stress in artificial freeze-tests—quick exposure to low temperatures with plant organs prone to flash freeze—differ from natural conditions where winter kill occurs due to prolonged exposure to sub-zero temperatures with severe freeze-induced dehydration stress (Gusta et al., 1997) or changing global climate change winter patterns (Willick et al., 2021). In addition, electrolyte leakage experiments are independent from intertwined factors that occur in nature and greatly impact field winter damage

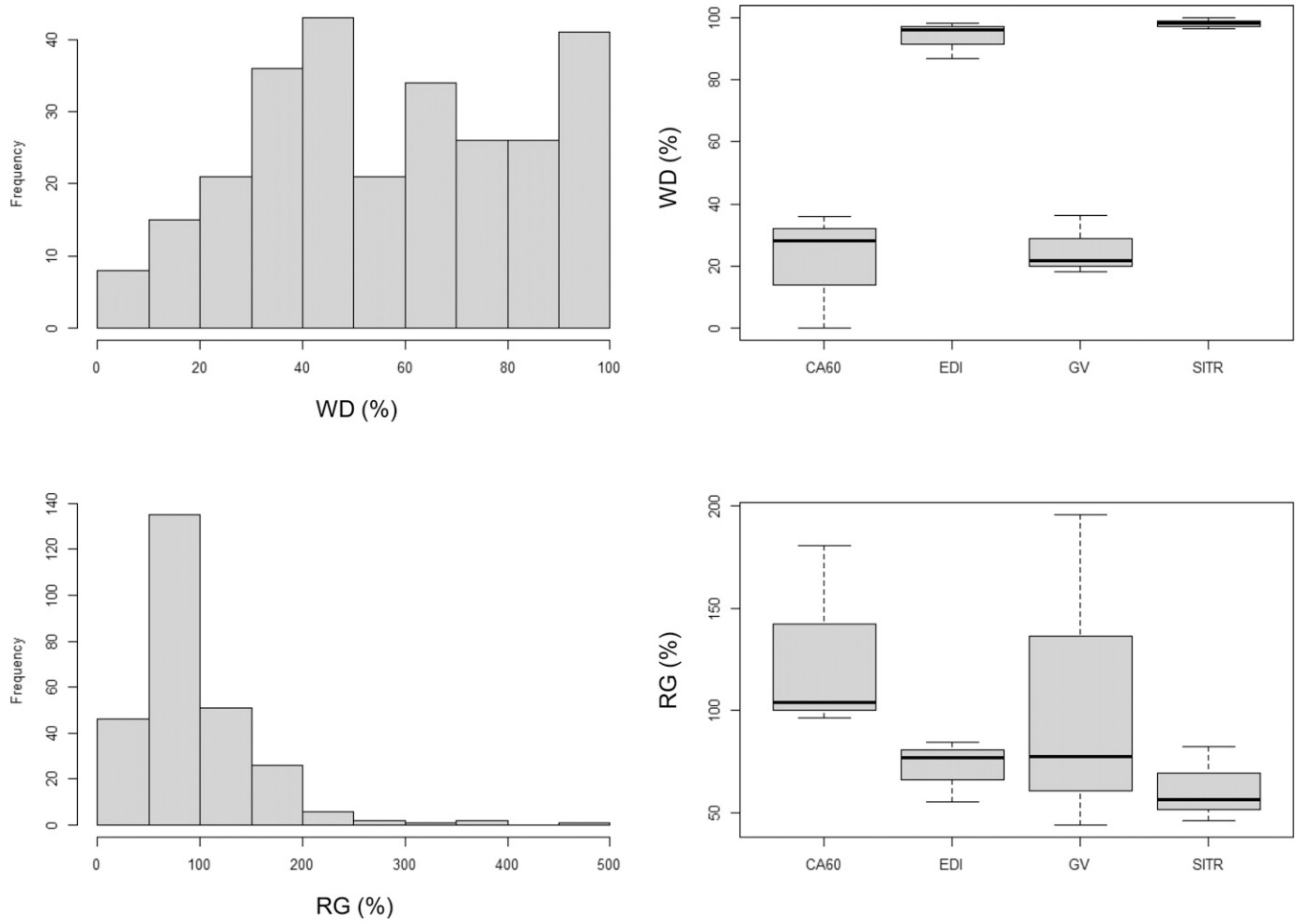

Fig. 8. Distribution of (**A**) field winter damage (WD) and (**B**) regrowth (RG) in the *Rosa* ×*hybrida* mapping population Easy Does It [EDI ('HARpageant')] × 'George Vancouver' (GV) and in *Rosa* ×*hybrida* genotypes CA60, EDI, GV, and CA60 × Singin' in the Rain™ [SITR ('MACivy')] at Elora, ON, Canada, in 2020. WD was a measurement of cane dieback in the field using the following formula: WD $(\%) = 100 \times \frac{ld}{lt}$, with WD being the percentage of winter damage, ld the length of dieback, and lt the length of the whole cane. RG was estimated with the following formula: RG $(\%) = 100 \times \frac{ln}{lt}$, with RG being the percentage of regrowth, ln the length of the new shoot, and lt the initial length of the whole cane. For both WD and RG, data on three canes per plant were collected and averaged.

ratings, such as overall plant health, pest pressure and soil status, carbohydrate allocation, and timing of acclimation and de-acclimation. Roses acclimate progressively in the fall until they reach their maximum level of winterhardiness midwinter and start to deacclimate. In a recent study, Ouyang et al. (2021) suggested that cold-hardy genotypes might acclimate faster and reach their maximum hardiness level earlier in the winter in comparison with nonhardy genotypes. Consequently, the multifactorial complex nature of field winter survival makes field trials the ultimate approach to measure field winterhardiness in roses, and only multiyear field testing can estimate winter survival (Karam and Sullivan, 1991).

As a result, despite the initial observations of electrolyte leakage being highly correlated with the USDA hardiness zones and field winterhardiness in a set of 28 commercial cultivars and elite genotypes, electrolyte leakage has limited utility to be used as a tool to select for hardy roses in a breeding program without the need for further field evaluation. Although electrolyte leakage and field winterhardiness data did not align for the breeding material, electrolyte leakage experiments are independent from the complex network of abiotic and biotic factors that occur in the field and could be relevant for the identification of candidate genes associated with freezing tolerance in roses. Electrolyte leakage experiments provide a reference point for a rose at a specific stage of its acclimation process as to the temperature below which injury will occur.

Distinct genetic basis of freezing tolerance under artificial stress and field winterhardiness

Given the lack of relationship between electrolyte leakage and winterhardiness, it was not surprising that the QTL for electrolyte leakage and field winterhardiness generally did not overlap. In addition, QTL for electrolyte leakage mapped to different genomic regions in the different parental maps; therefore, the action of complementary genes could explain the transgressive segregation. A total of seven QTL were identified for electrolyte leakage across mapping populations (Table 4). QTL for electrolyte leakage at −20 °C were located on LG2 in the CA60 × 'SITR' mapping population, and both parents contributed favorable alleles to freezing tolerance. Using the relative position of the molecular markers in the *R. chinensis* genome to survey the genome for potential candidate genes in this region, the QTL for electrolyte leakage at −20 °C on LG2 mapped nearby a key regulator of winterhardiness: the

Table 7. Correlation among best linear unbiased prediction estimates (BLUPs) of winter damage (WD), electrolyte leakage (EL), and LT50 for the *Rosa* ×*hybrida* mapping populations CA60 × Singin' in the Rain™ ['SITR' ('MACivy')] and Easy Does It™ ['EDI' ('HARpageant')] × 'George Vancouver' ('GV'). Pearson correlation coefficients are indicated, and significant correlation at $P = 0.05$, $P = 0.01$, and $P = 0.001$ are indicated by *, **, and ***, respectively.

	EL (%)							
	10 °C	15 °C	20 °C	25 °C	30 °C	35 °C	40 °C	LT50 (°C)[z]
1. CA60 × 'SITR' population								
WD Elora 2019[y]	0.08	0.26**	0.35***					
WD Elora 2020	−0.03	0.08	0.19*					
WD Sask 2019	0.26**	0.26**	0.31***					
2. 'EDI' × 'GV' population								
WD Elora 2020		0.13	0.20	0.25*	0.14	0.15	0.14	0.09

[z]The lethal temperature for which 50% of the plants are dead (LT50) was estimated for each genotype using a logit model approach.
[y]WD was a measurement of cane dieback using the following formula: $WD\ (\%) = 100 \times \frac{ld}{lt}$, with WD being the percentage of winter damage, ld the length of dieback, and lt the length of the whole cane. WD data were collected from four environments consisting of two locations (Elora, ON, Canada; Saskatoon, SK, Canada) and 2 years (2019–20) (Elora 2019, Elora 2020, Sask 2019, and Sask 2020). Sask 2020 was not used in this correlation, as no segregation was observed in the population because of too extreme climatic conditions.

ICE1-transcription factor (Supplemental Table 8). *ICE* is an upstream transcription factor of *CBF* genes with a major regulatory role in the acquisition of cold tolerance within the *CBF* pathway (Chinnusamy et al., 2003). A QTL for electrolyte leakage at −10 °C mapped to a different linkage group in the CA60 female map, suggesting that temperature-specific QTL for electrolyte leakage may exist, and this could be directly related to the cascade of activation and degradation of various genetic factors involved in the acquisition of freezing tolerance. The QTL mapped to a genomic region that harbors a *CBF1*-like transcription factor (Table 4, Supplemental Table 8). *CBF*-transcription factors are considered master regulators of cold hardiness (Wisniewski et al., 2014). They are overexpressed shortly after the perception of the cold signal before being degraded, and they activate downstream the expression of several *COR*-genes. QTL for electrolyte leakage at −20 °C mapped to LG6 in the 'EDI' female map, and it mapped to LG7 in the 'GV' male map.

QTL for winter damage

QTL were mapped for each environment separately. No stable QTL were identified. Although a QTL for winter damage in Elora 2019 was detected on LG2 in CA60, the QTL for winter damage in Elora 2020 mapped to LG1. Furthermore, although the QTL for electrolyte leakage at −20 °C and for winter damage in Elora 2019 did not collocate, they overlapped on LG2. A minor QTL for winter damage in Elora 2019 was identified in 'SITR' on LG5. In addition, a QTL for winter damage in Elora 2020 mapped to LG5 in the 'GV' male map. Although cold-hardy Explorer rose 'GV' contributed a favorable allele to winterhardiness, cold-sensitive floribunda 'SITR' carried a deleterious allele (Table 4). These results were consistent with expectations from a recent study conducted on genetic diversity between cold-hardy Canadian roses and non–cold-hardy European roses and between cold-hardy European roses and non–cold-hardy Canadian roses that suggested that LG5 would be a potential location for a QTL associated with winterhardiness (Vukosavljev, 2014). Similarly, QTL for winter damage in Elora 2020 in 'EDI' mapped to LG6, which was in agreement with Vukosavljev (2014), who indicated the presence of QTL associated with cold hardiness on LG6 of the non–cold-hardy large-flowered climber 'Red New Dawn'.

QTL for regrowth

Regrowth was inherited independently from winter damage, as the QTL for regrowth generally did not overlap with the QTL for winterhardiness. QTL for regrowth mapped to LG6 in the CA60 × 'SITR' population, whereas they mapped to LG2 and LG5 in the 'EDI' × 'GV' population. Exploration of the QTL intervals revealed the presence of numerous genes with gene ontology (GO) terms associated with cellular components and biological processes. GO terms associated with cellular components included plant-type cell wall organization, cell wall modification, and plasma membrane. GO terms associated with biological processes related to plant growth included carbohydrate metabolic process, phloem and xylem histogenesis, cell wall macromolecule catabolic process, cellulose biosynthetic process, seed development, and flower development. Further research is needed to examine patterns of gene expression in rose-development stages across environments (Walls et al., 2019).

Genetics of winterhardiness and regrowth

Winter damage is a quantitative trait under polygenic control. It is highly heritable but subject to GE interaction. The heritability estimates were comparable between the CA60 × 'SITR' population in Elora 2019 ($H^2 = 0.83$) and the 'EDI' × 'GV' population in Elora 2020 ($H^2 = 0.81$), and they were high (Table 6). These heritability estimates were also comparable to those found by Svejda (1979). However, the heritability of winter damage was low in Elora 2020 ($H^2 = 0.29$) and Sask 2019 ($H^2 = 0.13$).

The CA60 × 'SITR' population was evaluated for field winter damage at two different locations (Elora, ON, Canada, and Saskatoon, ON, Canada) featuring different climates (USDA zones 3b and 5b). Overall, winters in Saskatoon were far colder than winters in Elora, with extended periods of sub-zero temperatures, and they did not offer much insulating snow cover during the colder months, making the plants more vulnerable to freezing wind chill and desiccation (Supplemental Fig. 8). Under these extreme conditions, the progeny expressed lower genetic potential in Saskatoon than in Elora (Mathew et al., 2018). The extreme conditions contributed to cause severe damage to most plants, reducing the genetic variance and the heritability of the trait from 0.83 in Elora 2019 to 0.13 in Sask 2019. Sask 2020 was the most severe environment in which most plants suffered extensive damage. Consequently, winter temperatures are not the only driver of GE interaction, but prolonged periods of sub-

zero temperatures, snow cover, precipitation, and late fall and early spring temperatures that impact acclimation and de-acclimation are also involved.

The extent of winter damage is directly affected by various climatic factors; however, it also relies heavily on the overall health of the plant. The discrepancy between Elora 2019 and Elora 2020 was most likely due to a severe defoliation mainly caused by black spot that occurred at the end of Aug. 2019 and that impaired the assessment of winterhardiness in 2020, as indicated by the high positive correlations between winter damage, regrowth, and defoliation (Table 5). In addition, the QTL associated with winter damage and regrowth in Elora 2020, and defoliation mapped to a region with a major known locus for black spot disease resistance, *Rdr1*, discovered in the *R. multiflora* hybrid 91/100–5 (Von Malek and Debener, 1998). In a complementary study on black spot disease resistance in the CA60 × 'SITR' population, susceptibility ratings were collected on the progeny in detached leaf assays using single spore inoculum, and a marker linked to the black spot resistance CA60 *Rdr1A* allele was developed (Rouet et al., 2019). The QTL associated with winter damage and regrowth in Elora 2020, and defoliation, mapped to the same location as the QTL of resistance to black spot and the CA60*Rdr1A* allele (Rouet et al., 2019). CA60 is derived from 91/104, itself derived from CT50–9, a colchicine doubled clone of *R. multiflora* of 88/124–46, and 91/100–5 is derived from CT50–4 another chromosome doubled clone of 88/124–46. Interestingly, the colchicine doubled plants CT50–9 and CT50–4 being from the same regenerant and most probably genetically identical, 91/104 can be considered as a full sib of the genotype 91/100–5 from which the *Rdr1* gene was characterized (Von Malek and Debener, 1998; T. Debener, personal communication). The phylogenetic relatedness between 'CA60' and 88/124–46 being confirmed, 'CA60' *Rdr1* is most probably of same origin as the *muRdr1* gene discovered in 91/100–5.

Black spot has been found to be correlated with overall plant performance, horticultural value, vigor, winter survival, and winter injury in several studies (Carlson-Nilsson and Davidson, 2009; Mackay et al., 2008; Zlesak et al., 2017). Black spot can be responsible for much of the field winter injury because it severely weakens the plants as they enter dormancy, so it is not surprising to have detected a QTL for black spot resistance in the heavily infected Elora 2020 trial. Severe defoliation may promote the growth of new shoots late in the season that will not be mature enough to acclimate properly and will have not had enough carbohydrate reserves to allocate to overwintering (Carlson-Nilsson and Davidson, 2009). Dhont et al. (2006) also showed that early fall defoliation reduces accumulation of carbohydrate reserves in perennial alfalfa associated with a reduction in spring regrowth. Consequently, the ability to create exceptionally winter-hardy roses depends on the ability to simultaneously breed for increased black spot disease resistance as well as winterhardiness and regrowth.

Explorer Series of roses can mostly withstand severe winter conditions and show good spring regrowth; however, the Parkland Series roses mostly dieback to the snow line or to the crown, before growing back from the crown in the spring from stored carbohydrate reserves. Therefore, different strategies exist for winter survival that complicate how rose breeders define and evaluate field winterhardiness across genotypes and breeding material. Winter survival does not only depend on the degree of damage that the plant suffered in the winter but also on its ability to resume meristematic activity in the spring. In this research, regrowth was highly heritable in both populations in single environments (Table 6); however, the heritability decreased in higher stress environments associated with severe pest pressure or severe climatic conditions. Regrowth was in the same range across Elora and Saskatoon (Table 3), but the plants grew much bigger in Elora than in Saskatoon. The average shoot length of a rose bush in Elora was 55 cm, with a maximum of 1 m; however, the average shoot length of a rose bush in Saskatoon was 20 cm only, up to 50 cm (data not shown). Although QTL for winter damage and regrowth mapped to different linkage groups for Elora 2019, they colocalized on LG6 for Sask 2019 (Supplemental Fig. 4). Although winter damage and regrowth were not correlated in Elora 2019 ($r = -0.06$) and were inherited separately, they were negatively correlated in Sask 2019 [$r = -0.25$ (Table 5)]. Although the correlation was small, these results suggested that the more damaged the plants were after the winter in Sask 2019, the less regrowth occurred in the spring. With extensive winter damage on the canes, the new growth from the crown may not have benefited from newly fixed carbon by emerging leaflets performing photosynthesis but rather relied solely on stored carbohydrate reserves. Notably, the extremely hot and dry summer at the time of planting in Saskatoon, followed by a particularly cold fall, might have 1) compromised the establishment of the root system and slowed the overall growth after planting; 2) contributed to a reduction in the accumulation of carbohydrate reserves in the same year; 3) compromised the successful entry into dormancy and into the first winter; and 4) compromised the regrowth during the following growing season due to limited carbohydrate reserves. These results highlight the inability of the roses in this study to express their maximum hardiness levels in extremely severe environments that impose extreme selective pressure. Although Elora (USDA hardiness zone 5b) was an appropriate environment to evaluate the progeny of a cross between a hardy and a tender rose as long as pest pressure remained under control, Saskatoon (USDA hardiness zone 3a) would be an optimum environment to evaluate the adaptability of seedlings originating from the cross between a hardy rose and a semihardy rose or between two hardy roses (Svejda, 1979). Perhaps regional testing would have been appropriate for the CA60 × 'SITR' population. Furthermore, although the progeny of the population CA60 × 'SITR' was planted on its own roots, the control genotypes were grafted on the rootstock *R. multiflora.* Several clones of 'GV' were planted on their own roots, and others were grafted. There were no significant differences in winter damage between 'GV' grafted and 'GV' on its own roots (Fig. 5). Therefore, no effect of rootstock on these roses for hardiness was reported in this research; the rootstock could have been a confounding factor. Effects on winterhardiness in roses have been reported with the use of *R. canina* rootstock (Buck, 1964; De Vries, 1993). Buck (1964) suggested that the positive effect of *R. canina* rootstock on winterhardiness on roses is caused by an incompatibility between the rootstock and the scion leading to the accumulation of starch in the canes. Richer et al. (2006) have shown that the rootstock *R. multiflora* can have an impact on the survivability of roses from the Explorer Series under extreme winters in the first years of establishment. Depending on the cultivar, the rootstock *R. multiflora* could be associated with higher mortality rate under severe winter conditions and less growth in the subsequent years compared with roses grown on their own roots (e.g., cultivars Frontenac and William Baffin), or increased vigor and growth after a few

losses in the first years of establishment (e.g., cultivar John Davis). Decreased vigor of the plant could be due to repetitive frost damage at the grafting point and lack of compatibility between the rootstock and the scion. In general, the cultivar and climatic conditions in which it will be grown (mild or extreme winter) could have an impact on the choice of the multiplication method, whether the cultivar will be grown on its own roots or grafted (Richer et al., 2006). Although there is an effect of the rootstock on plant vigor, the blackspot tolerance of the *R. multiflora* rootstocks is not transmitted to the scion (Buck, 1964).

This research emphasizes on two key strategies of winter survival. The first strategy involves the successful entry into dormancy and into the first winter with the acquisition of winterhardiness. It relies on the accumulation of carbohydrate reserves and the timing of dormancy and growth cessation, and it is directly affected by the overall health of the plant, meaning that disease resistance is a critical feature. The second strategy corresponds to the regrowth after winter. It relies on the ability of the rose bush to not rely entirely on stored carbon reserves but also on newly fixed carbon by new leaflets performing photosynthesis, and it is dependent on bud survival on the canes.

Conclusions

Although electrolyte leakage was used as a proxy for field winterhardiness in a set of extremely differing commercial and elite roses, it had limited utility in the breeding material as a substitute to field trials for the target environments of this study. Winter damage is a quantitative trait under polygenic control, with parental genotypes contributing different alleles and mechanisms for winterhardiness. It was highly heritable, yet subjected to GE interactions, and no QTL for winter damage stable across locations were detected. The climate in Saskatoon, particularly in 2020, was too extreme for the roses to express their maximum hardiness levels observed under favorable conditions; therefore, as an environment, Saskatoon had limited ability to discriminate the genotypes of this study on the basis of hardiness levels. In addition, both winter damage and spring regrowth were affected by disease pressure. Breeding roses with increased winterhardiness clearly requires the breeder to simultaneously breed for disease resistance.

Literature Cited

Akhtar, M., A. Jaiswal, G. Taj, J.P. Jaiswal, M.I. Qureshi, and N.K. Singh. 2012. DREB1/CBF transcription factors: Their structure, function, and role in abiotic stress tolerance in plants. J. Genet. 91:385–395, https://doi.org/10.1007/s12041-012-0201-3.

Arends, D., P. Prins, R.C. Jansen, and K.W. Broman. 2010. R/Qtl: High-throughput multiple QTL mapping. Bioinformatics 26:2990–2992, https://doi.org/10.1093/bioinformatics/btq565.

Bąjji, M., J.M. Kinet, and S. Lutts. 2002. The use of the electrolyte leakage method for assessing cell membrane stability as a water stress tolerance test in durum wheat. Plant Growth Regulat. 36:61–70, https://doi.org/10.1023/A:1014732714549.

Barros, P.M., N. Gonçalves, N.J.M. Saibo, and M. Margarida Oliveira. 2012. Functional characterization of two almond C-repeat-binding factors involved in cold response. Tree Physiol. 32:1113–1128, https://doi.org/10.1093/treephys/tps067.

Bélanger, G., Y. Castonguay, A. Bertrand, C. Dhont, P. Rochette, L. Couture, R. Drapeau, D. Mongrain, F.P. Chalifour, and R. Michaud. 2006. Winter damage to perennial forage crops in eastern Canada: Causes, mitigation, and prediction. Can. J. Plant Sci. 86:33–47, https://doi.org/10.4141/P04-171.

Broman, K.W., D.M. Gatti, P. Simecek, N.A. Furlotte, P. Prins, Ś. Sen, B.S. Yandell, and G.A. Churchill. 2019. R/Qtl2: Software for mapping quantitative trait loci with high-dimensional data and multiparent populations. Genetics 211:495–502, https://doi.org/10.1534/genetics.118.301595.

Broman, K.W., H. Wu, Ś. Sen, and G.A. Churchill. 2003. R/Qtl: QTL mapping in experimental crosses. Bioinformatics 19:889–890, https://doi.org/10.1093/bioinformatics/btg112.

Buck, G.J. 1964. Stock-scion relationships in roses. Am. Rose Annu. 49:159–164.

Carlson-Nilsson, B.U. and C.G. Davidson. 2009. A three-year study of winter hardiness and blackspot resistance (*Diplocaron rosae* Wolf) of roses in two climatically different environments. Floric. Ornam. Biotechnol. 3:139–151, https://doi.org/10.1016/j.scienta.2018.10.003.

Chinnusamy, V., M. Ohta, S. Kanrar, B.H. Lee, X. Hong, M. Agarwal, and J.K. Zhu. 2003. ICE1: A regulator of cold-induced transcriptome and freezing tolerance in *Arabidopsis*. Genes Dev. 17:1043–1054, https://doi.org/10.1101/gad.1077503.

De Vries, D.P. 1993. The vigour of glasshouse roses: Scion-rootstock relationships: Effects of phenotypic and genotypic variation. Wageningen Univ., Wageningen, Neth.

Dexter, S.T., W.E. Tottingham, and L.F. Graber. 1930. Preliminary results in measuring the hardiness of plants. Plant Physiol. 5:215–223, https://doi.org/10.1104/pp.5.2.215.

Dhont, C., Y. Castonguay, P. Nadeau, G. Bélanger, R. Drapeau, S. Laberge, J.C. Avice, and F.P. Chalifour. 2006. Nitrogen reserves, spring regrowth and winter survival of field-grown alfalfa (*Medicago sativa)* defoliated in the autumn. Ann. Bot. 97:109–120, https://doi.org/10.1093/aob/mcj006.

Dumont, E., V. Fontaine, C. Vuylsteker, H. Sellier, S. Bodèle, N. Voedts, R. Devaux, M. Frise, A. Komlan, J.L. Hilbert, B. Nasser, E. Hanocq, I. Lejeune-Hénaut, and B. Delbreil. 2009. Association of sugar content QTL and PQL with physiological traits relevant to frost damage resistance in pea under field and controlled conditions. Theor. Appl. Genet. 118:1561–1571, https://doi.org/10.1007/s00122-009-1004-7.

Environment Canada. Historical data. 15 Mar. 2021. https://climate.weather.gc.ca/historical_data.

Frutos, E., M. Purificación Galindo, and V. Leiva. 2014. An interactive biplot implementation in R for modeling genotype-by-environment interaction. Stochastic Environ. Res. Risk Assess. 28:1629–1641, https://doi.org/10.1007/s00477-013-0821-z.

Gery, C., E. Zuther, E. Schulz, J. Legoupi, A. Chauveau, H. McKhann, D.K. Hincha, and E. Téoulé. 2011. Natural variation in the freezing tolerance of *Arabidopsis thaliana*: Effects of rnai-induced CBF depletion and QTL localisation vary among accessions. Plant Sci. 180:12–23, https://doi.org/10.1016/j.plantsci.2010.07.010.

Gitonga, V.W., C.F.S. Koning-Boucoiran, K. Verlinden, O. Dolstra, R. Visser, C. Maliepaard, and F.A. Krens. 2014. Genetic variation, heritability, and genotype by environment interaction of morphological traits in a tetraploid rose population. BMC Genet. 15:146, https://doi.org/10.1186/s12863-014-0146-z.

Gusta, L.V., B.J. O'Connor, and M.G. MacHutcheon. 1997. The selection of superior winter-hardy genotypes using a prolonged freeze test. Can. J. Plant Sci. 77:15–21, https://doi.org/10.4141/P95-197.

Guy, C.L. 1990. Cold acclimation and freezing stress tolerance: Role of protein metabolism. Plant Mol. Biol. 41:187–223, https://doi.org/10.1146/annurev.pp.41.060190.001155.

Haley, C.S. and S.A. Knott. 1992. A simple regression method for mapping quantitative trait loci in line crosses using flanking markers. Heredity (Edinb.) 69:315–324, https://doi.org/10.1038/hdy.1992.131.

Kalcsits, L.A., S. Silim, and K.K. Tanino. 2009. Warm temperature accelerates short photoperiod-induced growth cessation and dormancy induction in hybrid poplar (*Populus* × spp.). Trees (Berl.) 23:971–979, https://doi.org/10.1007/s00468-009-0339-7.

Karam, F.H. and J.A. Sullivan. 1991. A rapid method for detection of cold hardiness in roses. HortScience 26:59–60, https://doi.org/10.21273/HORTSCI.26.1.59.

Kitashiba, H., T. Ishizaka, K. Isuzugawa, K. Nishimura, and T. Suzuki. 2004. Expression of a sweet cherry DREB1/CBF ortholog in

Arabidopsis confers salt and freezing tolerance. J. Plant Physiol. 161:1171–1176, https://doi.org/10.1016/j.jplph.2004.04.008.
Le, L., M. Rui, X.F. Sun, W. Qiong, L. Hui, H.T. Pan, and Q.X. Zhang. 2012. Preliminary studies on cold resistance evaluation of modern roses. Acta Hort. (9372):889–900, https://doi.org/10.17660/ACTAHORTIC.2012.937.109.
Li, X., Y. Wei, A. Acharya, Q. Jiang, J. Kang, and E.C. Brummer. 2014. A saturated genetic linkage map of autotetraploid alfalfa (*Medicago sativa* L.) developed using genotyping-by-sequencing is highly syntenous with the *Medicago truncatula* genome. G3 (Bethesda) 4:1971–1979, https://doi.org/10.1534/g3.114.012245.
Lindén, L., P. Palonen, and M. Lindén. 2000. Relating freeze-induced electrolyte leakage measurements to lethal temperature in red raspberry. J. Amer. Soc. Hort. Sci. 125:429–435, https://doi.org/10.21273/JASHS.125.4.429.
Ling, J., Y. Xiao, J. Hu, F. Wang, F. Ouyang, J. Wang, Y. Weng, and H. Zhang. 2021. Genotype-by-environment interaction analysis of growth of *Picea koraiensis* families at different sites using BLUP-GGE. New Forests 52:113–127, https://doi.org/10.1007/s11056-020-09785-3.
Mackay, W.A., S.W. George, C. McKenney, J.J. Sloan, R.I. Cabrera, J.A. Reinert, P. Colbaugh, L. Lockett, and W. Crow. 2008. Performance of garden roses in north-central Texas under minimal input conditions. HortTechnology 18:417–422, https://doi.org/10.21273/HORTTECH.18.3.417.
von Malek, B. and T. Debener. 1998. Genetic analysis of resistance to blackspot (*Diplocarpon rosae*) in tetraploid roses. Theor. Appl. Genet. 96:228–231, https://doi.org/10.1007/s001220050731.
Mathew, I., H. Shimelis, L. Mwadzingeni, R. Zengeni, M. Mutema, and V. Chaplot. 2018. Variance components and heritability of traits related to root: Shoot biomass allocation and drought tolerance in wheat. Euphytica 214:225, https://doi.org/10.1007/s10681-018-2302-4.
Nakagawa, S. and H. Schielzeth. 2010. Repeatability for Gaussian and non-Gaussian data: A practical guide for biologists. Biol. Rev. Camb. Philos. Soc. 85:935–956, https://doi.org/10.1111/j.1469-185X.2010.00141.x.
Novillo, F., J. Medina, and J. Salinas. 2007. *Arabidopsis* CBF1 and CBF3 have a different function than CBF2 in cold acclimation and define different gene classes in the CBF regulon. Proc. Natl. Acad. Sci. USA 104:21002–21007, https://doi.org/10.1073/pnas.0705639105.
Ogilvie, I.S., and Agriculture Canada Communications Branch. 1993. Winter-hardy roses. Agriculture Canada, Ottawa, ON, Canada.
Ouyang, L., L. Leus, E. De Keyser, and M.C. Van Labeke. 2019. Seasonal changes in cold hardiness and carbohydrate metabolism in four garden rose cultivars. J. Plant Physiol. 232:188–199, https://doi.org/10.1016/j.jplph.2018.12.001.
Ouyang, L., L. Leus, and M.C. Van Labeke. 2019. Three-year screening for cold hardiness of garden roses. Scientia Hort. 245:12–18, https://doi.org/10.1016/j.scienta.2018.10.003.
Ouyang, L., L. Leus, E. De Keyser, and M.C. Van Labeke. 2021. Dehydrins and soluble sugars involved in cold acclimation of *Rosa wichurana* and rose cultivar 'Yesterday'. Horticulturae 10:379, https://doi.org/10.3390/horticulturae7100379.
Peixoto, M.D.M. and R.F. Sage. 2016. Improved experimental protocols to evaluate cold tolerance thresholds in *Miscanthus* and switchgrass rhizomes. Glob. Change Biol. Bioenergy 8:257–268, https://doi.org/10.1111/gcbb.12301.
Poirier, M., A. Lacointe, and T. Améglio. 2010. A semi-physiological model of cold hardening and dehardening in walnut stem. Tree Physiol. 30:1555–1569, https://doi.org/10.1093/treephys/tpq087.
Raymond, O., J. Gouzy, J. Just, H. Badouin, M. Verdenaud, A. Lemainque, P. Vergne, S. Moja, N. Choisne, C. Pont, S. Carrère, J.C. Caissard, A. Couloux, L. Cottret, J.M. Aury, J. Szécsi, D. Latrasse, M.A. Madoui, L. François, X. Fu, S.H. Yang, A. Dubois, F. Piola, A. Larrieu, M. Perez, K. Labadie, L. Perrier, B. Govetto, Y. Labrousse, P. Villand, C. Bardoux, V. Boltz, C. Lopez-Roques, P. Heitzler, T. Vernoux, M. Vandenbussche, H. Quesneville, A. Boualem, A. Bendahmane, C. Liu, M. Le Bris, J. Salse, S. Baudino, M. Benhamed, P. Wincker, and M. Bendahmane. 2018. The *Rosa* genome provides new insights into the domestication of modern roses. Nat. Genet. 50:772–777, https://doi.org/10.1038/s41588-018-0110-3.
Richer, C., J.A. Rioux, M.P. Lamy, and R. Drapeau. 2006. Impact de la méthode de multiplication sur la croissance de 10 rosiers de la Série Explorateur^{MC} soumis à des conditions hivernales naturelles et extremes. Can. J. Plant Sci. 86:799–807. https://doi-org.subzero.lib.uoguelph.ca/10.4141/P05-021.
Rouet, C., E.A. Lee, T. Banks, J. O'Neill, R. LeBlanc, and D.J. Somers. 2019. Identification of a polymorphism within the *Rosa multiflora* MuRdr1A gene linked to resistance to multiple races of *Diplocarpon rosae* W. in tetraploid garden roses (*Rosa ×hybrida*). Theor. Appl. Genet. 133:103–117, https://doi.org/10.1007/s00122-019-03443-9.
Saskatchewan Research Council. 2021. Climate reference stations. 15 Mar. 2021. www.src.sk.ca/labs/climate-reference-stations.
Săulescu, N.N. and H.J. Braun. 2001. Cold tolerance, p 111–123. In: M.P. Reynold, J.I. Ortiz-Monasterio, and A. McNab (eds.). Application of physiology in wheat breeding. Cimmyt, Mexico City, Mexico.
Spiller, M., M. Linde, L. Hibrand-Saint Oyant, C.J. Tsai, D.H. Byrne, M.J.M. Smulders, F. Foucher, and T. Debener. 2011. Towards a unified genetic map for diploid roses. Theor. Appl. Genet. 122:489–500, https://doi.org/10.1007/s00122-010-1463-x.
Svejda, F. 1979. Inheritance of winterhardiness in roses. Euphytica 28:309–314, https://doi.org/10.1007/BF00056587.
Svejda, F. 2008. The Canadian Explorer Roses. National Roses Canada, London, ON, Canada.
Taylor, J. and D. Butler. 2017. R package ASMap: EEficient genetic linkage map construction and diagnosis. J. Stat. Softw. 79: https://doi.org/10.18637/jss.v079.i06.
Vukosavljev, M. 2014. Towards marker assisted breeding in garden roses: From marker development to QTL detection. 16 May. 2022. http://edepot.wur.nl/318534.
Walls, R.L., L. Cooper, J. Elser, M.A. Gandolfo, C.J. Mungall, B. Smith, D.W. Stevenson, and P. Jaiswal. 2019. The plant ontology facilitates comparisons of plant development stages across species. Front. Plant Sci. 10:631, https://doi.org/10.3389/fpls.2019.00631.
Wickham, H. 2016. ggplot2: Elegant graphics for data analysis. Springer, Cham, Switzerland. https://doi-org.subzero.lib.uoguelph.ca/10.1007/978-3-319-24277-4.
Willick, I.R., K.K. Tanino, and L.V. Gusta. 2021. The impact of global climate change on the freezing tolerance of winter cereals in western Canada. J. Agron. Crop Sci. 201:88–99, https://doi.org/10.1111/jac.12447.
Willick, I.R., L.V. Gusta, B.D. Fowler, and K.K. Tanino. 2019. Ice segregation in the crown of winter cereals: Evidence for extraorgan and extratissue freezing. Plant Cell Environ. 42:701–716, https://doi.org/10.1111/pce.13454.
Wisniewski, M., A. Nassuth, C. Teulières, C. Marque, J. Rowland, P.B. Cao, and A. Brown. 2014. Genomics of cold hardiness in woody plants. Crit. Rev. Plant Sci. 33:92–124, https://doi.org/10.1080/07352689.2014.870408.
Wisniewski, M., J. Norelli, C. Bassett, T. Artlip, and D. Macarisin. 2011. Ectopic expression of a novel peach (*Prunus persica*) CBF transcription factor in apple (*Malus ×domestica*) results in short-day induced dormancy and increased cold hardiness. Planta 233:971–983, https://doi.org/10.1007/s00425-011-1358-3.
Zhao, K., Y. Zhou, Y. Li, X. Zhuo, S. Ahmad, Y. Han, X. Yong, and Q. Zhang. 2018. Crosstalk of PmCBFs and PmDAMs based on the changes of phytohormones under seasonal cold stress in the stem of *Prunus mume*. Int. J. Mol. Sci. 19:15, https://doi.org/10.3390/ijms19020015.
Zlesak, D. 2007. Rose: *Rosa ×hybrida*, p. 695–740. In: N.O. Anderson (ed.). Flower breeding and genetics. Springer, Heidelberg, Gemany. https://doi-org.subzero.lib.uoguelph.ca/10.1007/978-1-4020-4428-1.
Zlesak, D., R. Nelson, D. Harp, B. Villarreal, N. Howell, J. Griffin, G. Hammond, and S. George. 2017. Performance of landscape roses grown with minimal input in the north-central, central, and south-central United States. HortTechnology 27:718–730, https://doi.org/10.21273/HORTTECH03681-17.

Supplemental Material

Data analysis of electrolyte leakage data

Statistical analysis was conducted separately for the parental lines {CA60, Singin' in the Rain ['SITR' ('MACivy')], Easy Does It ['EDI' ('HARpageant')], and 'George Vancouver' ('GV')} and the two mapping populations CA60 × 'SITR' and 'EDI' × 'GV'. General linear mixed models (GLMMs) were fitted on the electrolyte leakage (EL) and index of injury (I) data collected in a split-plot design using statistical software (SAS version 9.4; SAS Institute Inc., Cary, NC). Replication was set as the factor Block, Temperature was the main-plot factor, and Genotype was allocated to subplot. EL and I data corresponded to a proportion measure and was defined as a non–Gaussian-dependent variable with a beta distribution. The logit function was used as the link function in the GLMM analysis.

Parental lines

The variance of EL and I was partitioned into fixed effects (temperature, genotype, temperature × genotype) and random effects (replication, replication × temperature, and replication × temperature × genotype). Thus, the linear predictor was defined as $\eta ij = \eta + b_i + \alpha_j + (ba)_{ij} + \tau_k + (bt)_{ik} + (\alpha\tau)_{jk} + (bat)_{ijk}$, where η is the intercept, b_i is the effect of block, α_j the effect of main treatment temperature, $(ba)_{ij}$ is the random effect of the whole-plot units involving factor temperature, τ_k the effect of the genotype, $(bt)_{ik}$ the random effect involving genotype, $(\alpha\tau)_{jk}$ the interaction effect between genotype and temperature, and $(bat)_{ijk}$ the error associated with the interaction of the effects at the whole-plot unit. A type I error of 0.05 was used to determine the significance of tests in this analysis. Variance analysis was performed using the GLIMMIX procedure with Laplace interval estimation. Type III tests of fixed effects were used in the variance analysis and random effects were tested with a likelihood test for covariance parameters. The fit of the models was investigated based on an analysis of the studentized conditional residuals. BLUE estimates of EL were computed for the parental genotypes CA60, 'SITR', 'EDI', and 'GV'.

CA60 × 'SITR' population

The variance of EL was partitioned into fixed effects (temperature) and random effects (replication, replication × temperature, genotype, temperature × genotype, and replication × temperature × genotype). Thus, the linear predictor was defined as $\eta ij = \eta + b_i + \alpha_j + (ba)_{ij} + \tau_k + (bt)_{ik} + (\alpha\tau)_{jk} + (bat)_{ijk}$, where η is the intercept, b_i is the effect of block, α_j the effect of main treatment temperature, $(ba)_{ij}$ is the random effect of the whole-plot units involving factor temperature, τ_k the effect of the genotype, $(bt)_{ik}$ the random effect involving genotype, $(\alpha\tau)_{jk}$ the interaction effect between genotype and temperature, and $(bat)_{ijk}$ the error associated with the interaction of the effects at the whole-plot unit. Best linear unbiased predictor (BLUP) estimates of EL were computed for each temperature.

'EDI' × 'GV' population

The variance of EL and I was partitioned into fixed effects (temperature) and random effects (replication, replication × temperature, genotype, temperature × genotype). The random effect replication × temperature × genotype was not included in this model because only one technical replication was available per biological replication of the EL assay. Thus, the linear predictors were defined as $\eta ij = \eta + b_i + \alpha_j + (ba)_{ij} + \tau_k + (bt)_{ik} + (\alpha\tau)_{jk}$, where η is the intercept, b_i is the effect of block, α_j the effect of main treatment temperature, $(ba)_{ij}$ is the random effect of the whole-plot units involving factor temperature, τ_k the effect of the genotype, $(bt)_{ik}$ the random effect involving genotype, and $(\alpha\tau)_{jk}$ the interaction effect between genotype and temperature. BLUP estimates of EL and I were computed for 'EDI' × 'GV'. BLUP estimates of EL were computed for each temperature.

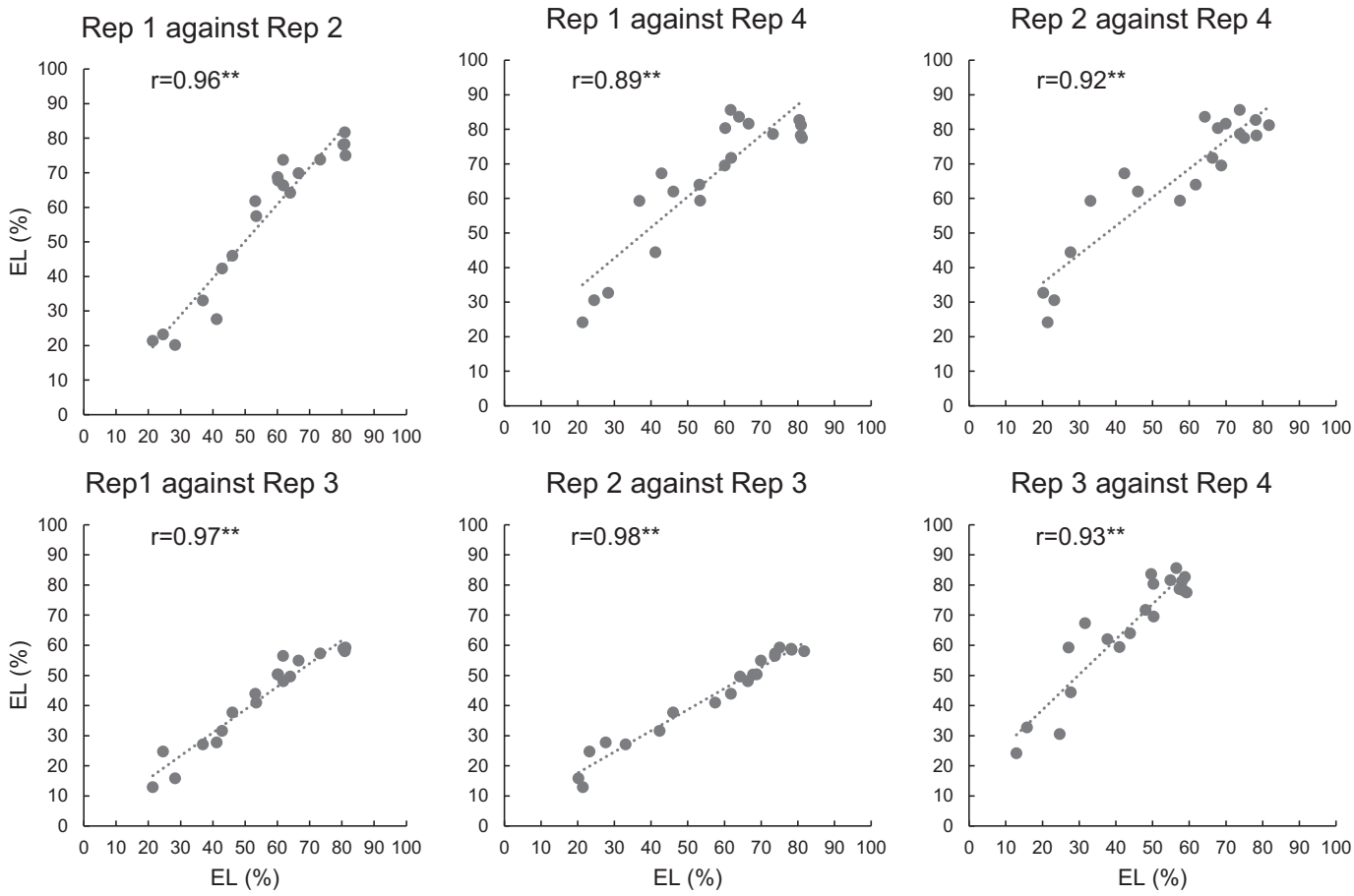

Supplemental Fig. 1. Comparison of magnitude of electrolyte leakage (EL) among four replications (Rep) of electrolyte leakage assays conducted on the hardy *Rosa* ×*hybrida* parental lines CA60 and 'George Vancouver' ('GV'). EL was recorded at 4 (i.e., control), −10, −15, −20, −25, −30, −35, −40, −45, and −50 °C. Correlations were computed using the Pearson method. Significant correlations are given with ** significant at $P = 0.001$.

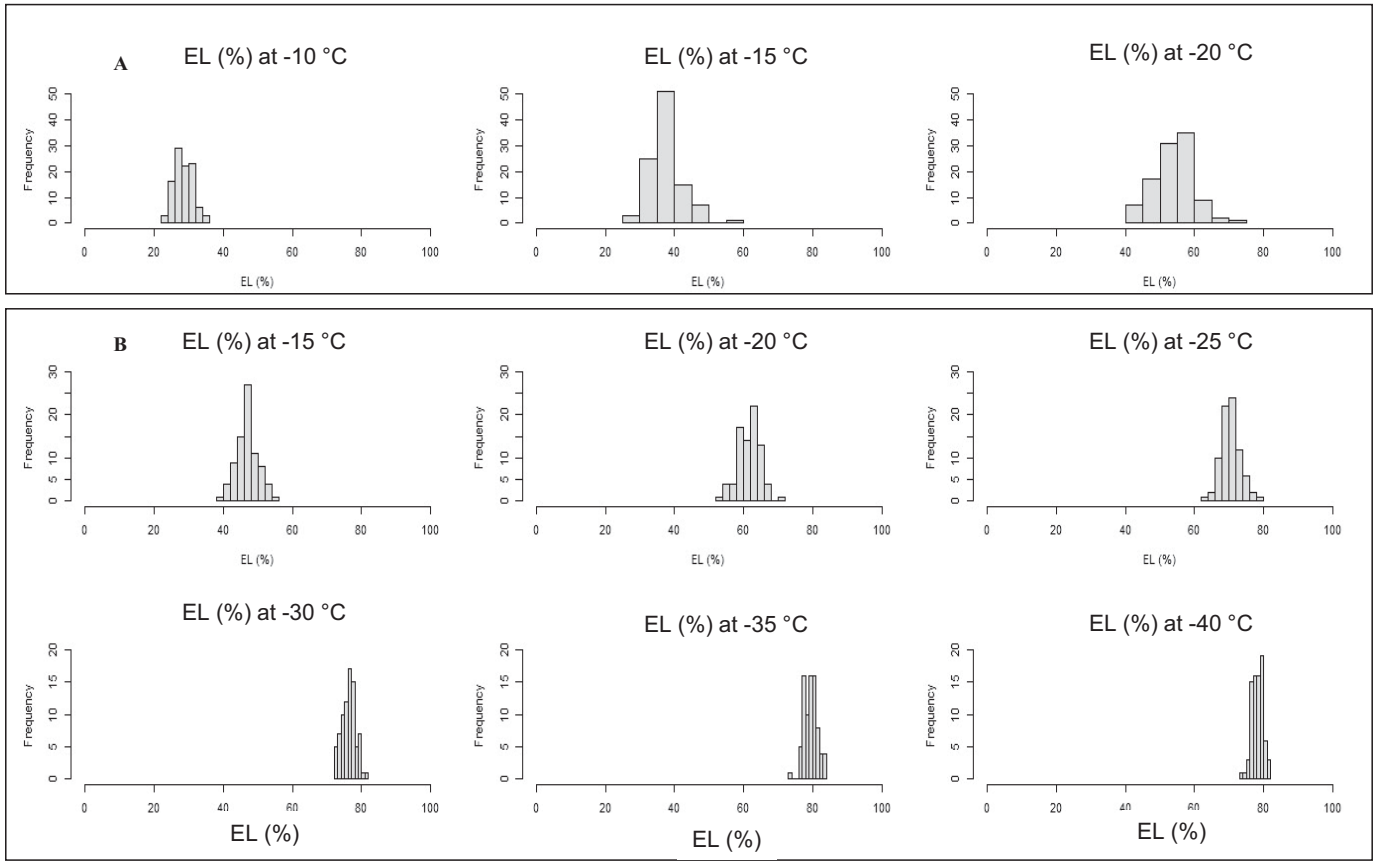

Supplemental Fig. 2. Distribution of best linear unbiased predictors (BLUPs) of electrolyte leakage (EL) (**A**) in the *Rosa* ×*hybrida* mapping population CA60 × Singin' in the Rain ['SITR' ('MACivy')] at −10, −15, and −20 °C and (**B**) in the *R.* ×*hybrida* mapping population Easy Does It ['EDI' ('HARpageant')] × 'George Vancouver' ('GV') at −15, −20, −25, −30, −35, and −40 °C.

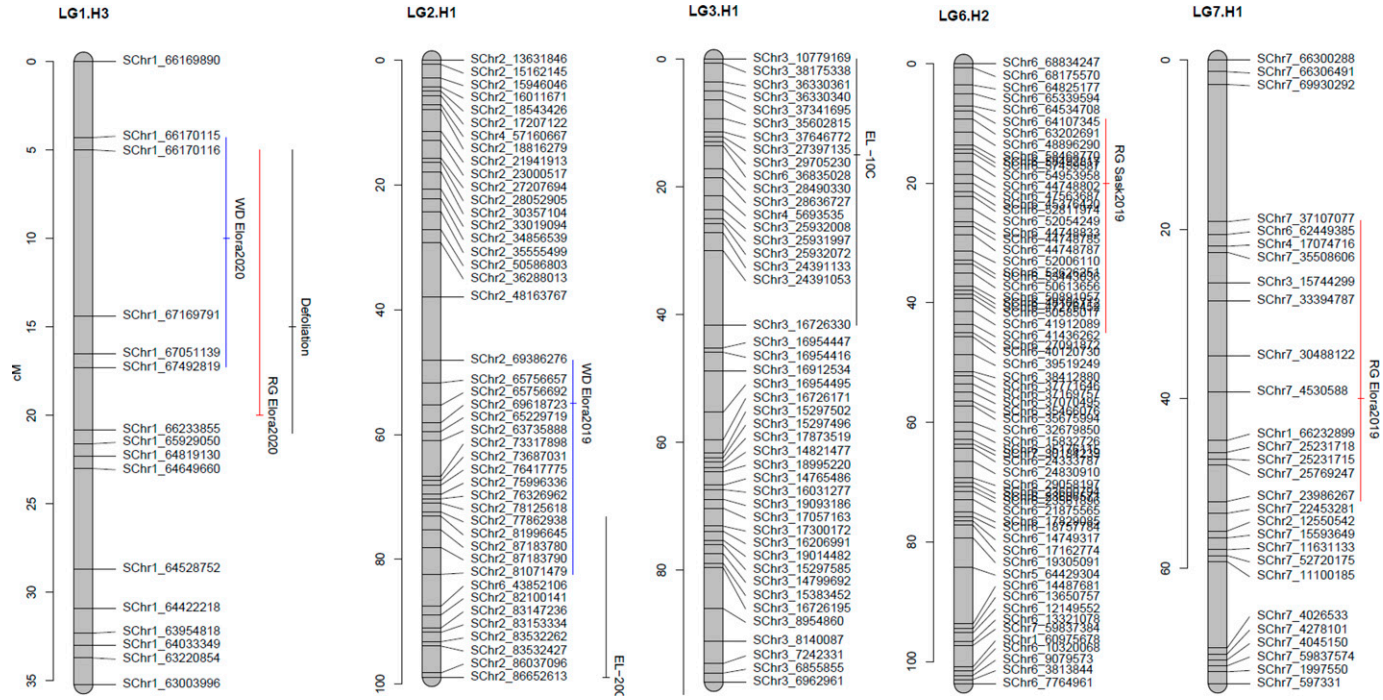

Supplemental Fig. 3. Quantitative trait loci (QTL) mapping of best linear unbiased predictors (BLUPs) of electrolyte leakage (EL) at −10 and −20 °C, field winter damage (WD) and field regrowth (RG) in four environments consisting of two locations (Elora, ON, Canada, and Saskatoon, SK, Canada) and 2 years (2019–20) (Elora 2019, Elora 2020, Sask 2019, and Sask 2020) in the genetic map of *Rosa ×hybrida* CA60. WD was a measurement of cane dieback using the following formula: WD $(\%) = 100 \times \frac{\text{ld}}{\text{lt}}$, with WD being the percentage of winter damage, ld the length of dieback, and lt the length of the whole cane. RG was estimated with the following formula: RG $(\%) = 100 \times \frac{\text{ln}}{\text{lt}}$, with RG being the percentage of regrowth, ln the length of the new shoot and lt the initial length of the whole cane. For both WD and RG, three stems per plant were measured and the average value for each plant was used as the final rating. The genetic markers were named based on their relative position in the reference genome *Rosa chinensis* (Raymond et al., 2018), and the nomenclature used for the linkage groups followed Spiller et al. (2011).

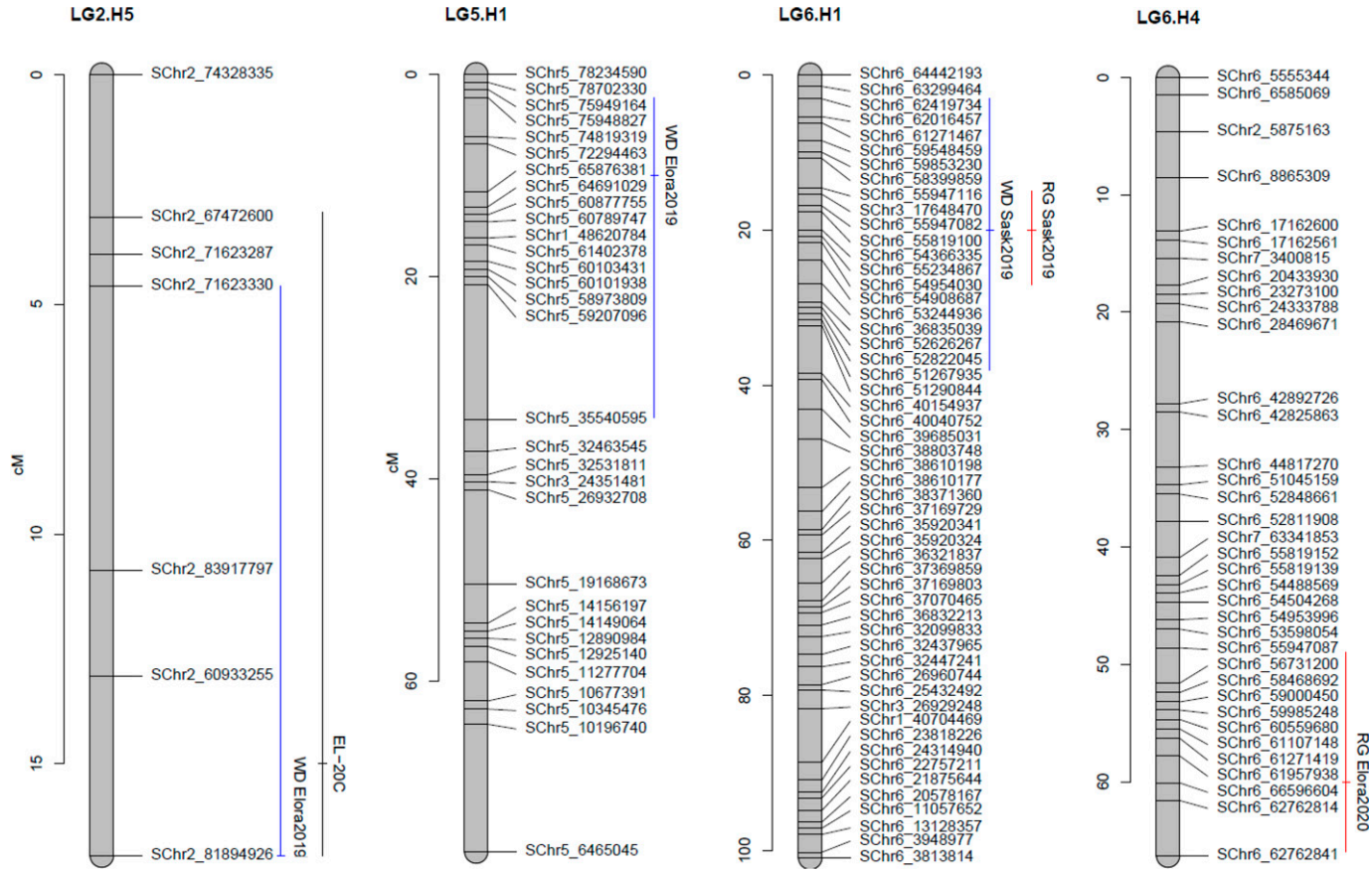

Supplemental Fig. 4. Quantitative trait loci (QTL) mapping of best linear unbiased predictors (BLUPs) of electrolyte leakage (EL) at −10 and −20 °C, field winter damage (WD), and field regrowth (RG) in four environments consisting of two locations (Elora, ON, Canada; Saskatoon, SK, Canada) and 2 years (2019–20) (Elora 2019, Elora 2020, Sask 2019, and Sask 2020) in the genetic map of *Rosa* ×*hybrida* Singin' in the Rain™ ['SITR' ('MACivy')]. WD was a measurement of cane dieback using the following formula: WD $(\%) = 100 \times \frac{ld}{lt}$, with WD being the percentage of winter damage, ld the length of dieback, and lt the length of the whole cane. RG was estimated with the following formula: RG $(\%) = 100 \times \frac{ln}{lt}$, with RG being the percentage of regrowth, ln the length of the new shoot, and lt the initial length of the whole cane. For both WD and RG, three stems per plant were measured and the average value for each plant was used as the final rating. The genetic markers were named based on their relative position in the reference genome *Rosa chinensis* (Raymond et al., 2018), and the nomenclature used for the linkage groups followed Spiller et al. (2011).

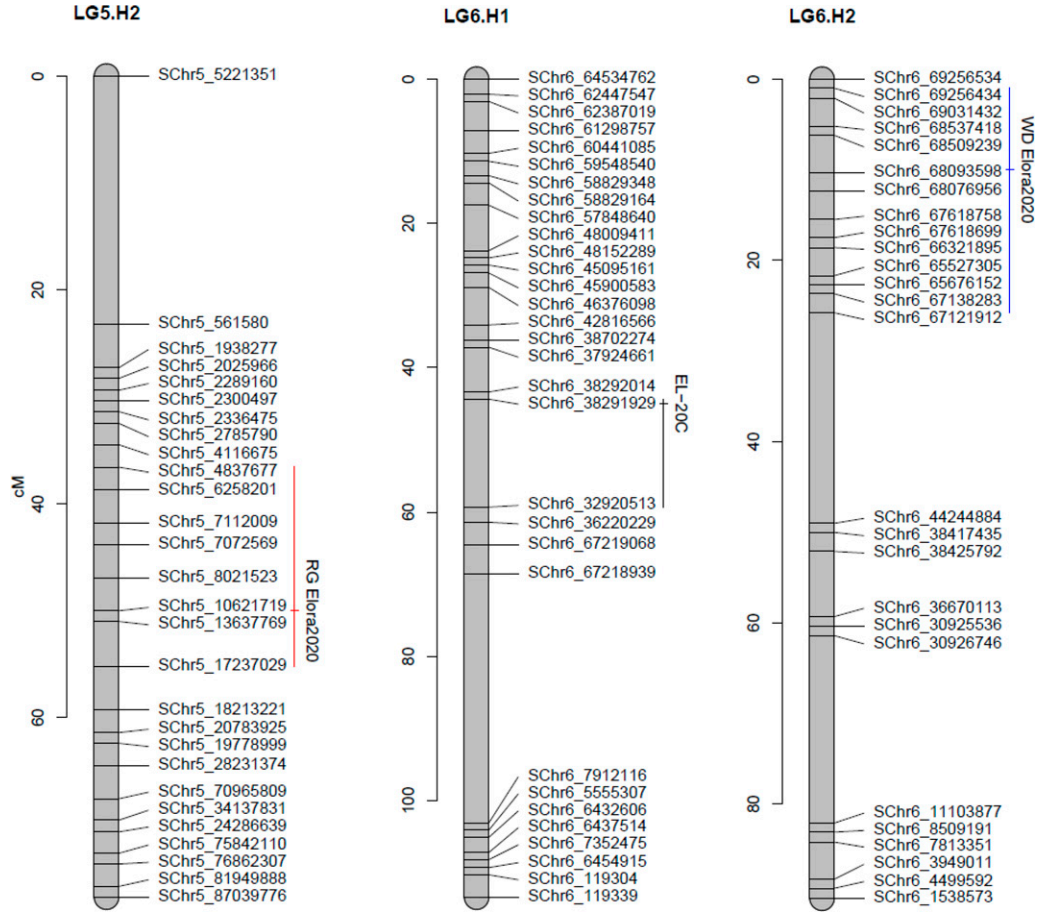

Supplemental Fig. 5. Quantitative trait loci (QTL) mapping of best linear unbiased predictors (BLUPs) of electrolyte leakage (EL) at −10 and −20 °C, field winter damage (WD), and field regrowth (RG) in Elora, ON, Canada, in 2020 (Elora 2020) in the genetic map of *Rosa* ×*hybrida* Easy Does It ['EDI' ('HARpageant')]. WD was a measurement of cane dieback using the following formula: WD $(\%) = 100 \times \frac{ld}{lt}$, with WD being the percentage of winter damage, ld the length of dieback, and lt the length of the whole cane. RG was estimated with the following formula: $RG\ (\%) = 100 \times \frac{ln}{lt}$, with RG being the percentage of regrowth, ln the length of the new shoot, and lt the initial length of the whole cane. For both WD and RG, three stems per plant were measured and the average value for each plant was used as the final rating. The genetic markers were named based on their relative position in the reference genome *Rosa chinensis* (Raymond et al., 2018), and the nomenclature used for the linkage groups followed Spiller et al. (2011).

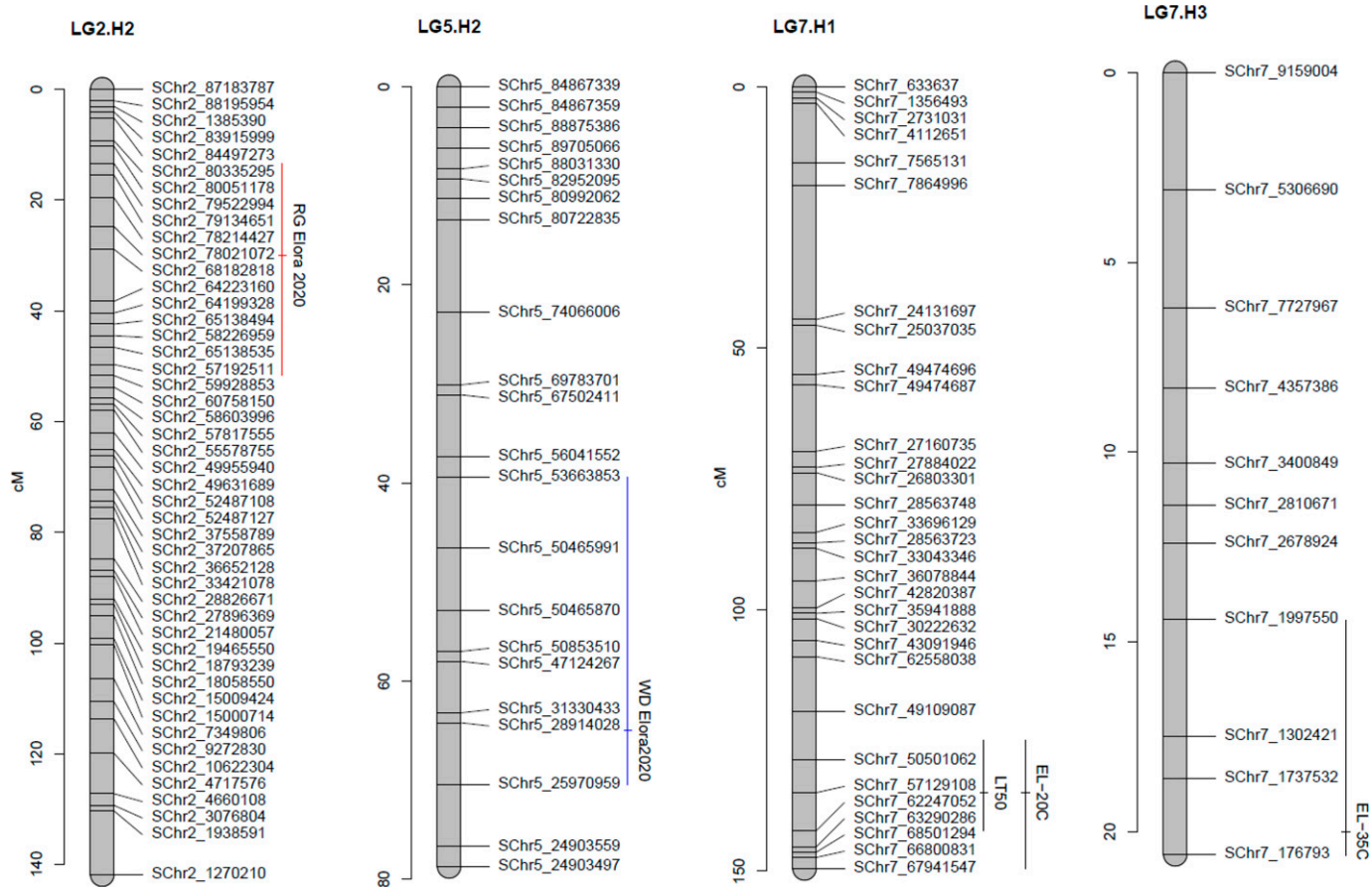

Supplemental Fig. 6. Quantitative trait loci (QTL) mapping of best linear unbiased predictors (BLUPs) of electrolyte leakage (EL) at −10 and −20 °C, field winter damage (WD), and field regrowth (RG) in Elora (ON, Canada) in 2020 (Elora 2020) in the genetic map of *Rosa* ×*hybrida* 'George Vancouver'('GV'). WD was a measurement of cane dieback using the following formula: WD $(\%) = 100 \times \frac{\text{ld}}{\text{lt}}$, with WD being the percentage of winter damage, ld the length of dieback, and lt the length of the whole cane. RG was estimated with the following formula: RG $(\%) = 100 \times \frac{\text{ln}}{\text{lt}}$, with RG being the percentage of regrowth, ln the length of the new shoot, and lt the initial length of the whole cane. For both WD and RG, three stems per plant were measured, and the average value for each plant was used as the final rating. The genetic markers were named based on their relative position in the reference genome *Rosa chinensis* (Raymond et al., 2018), and the nomenclature used for the linkage groups followed Spiller et al. (2011).

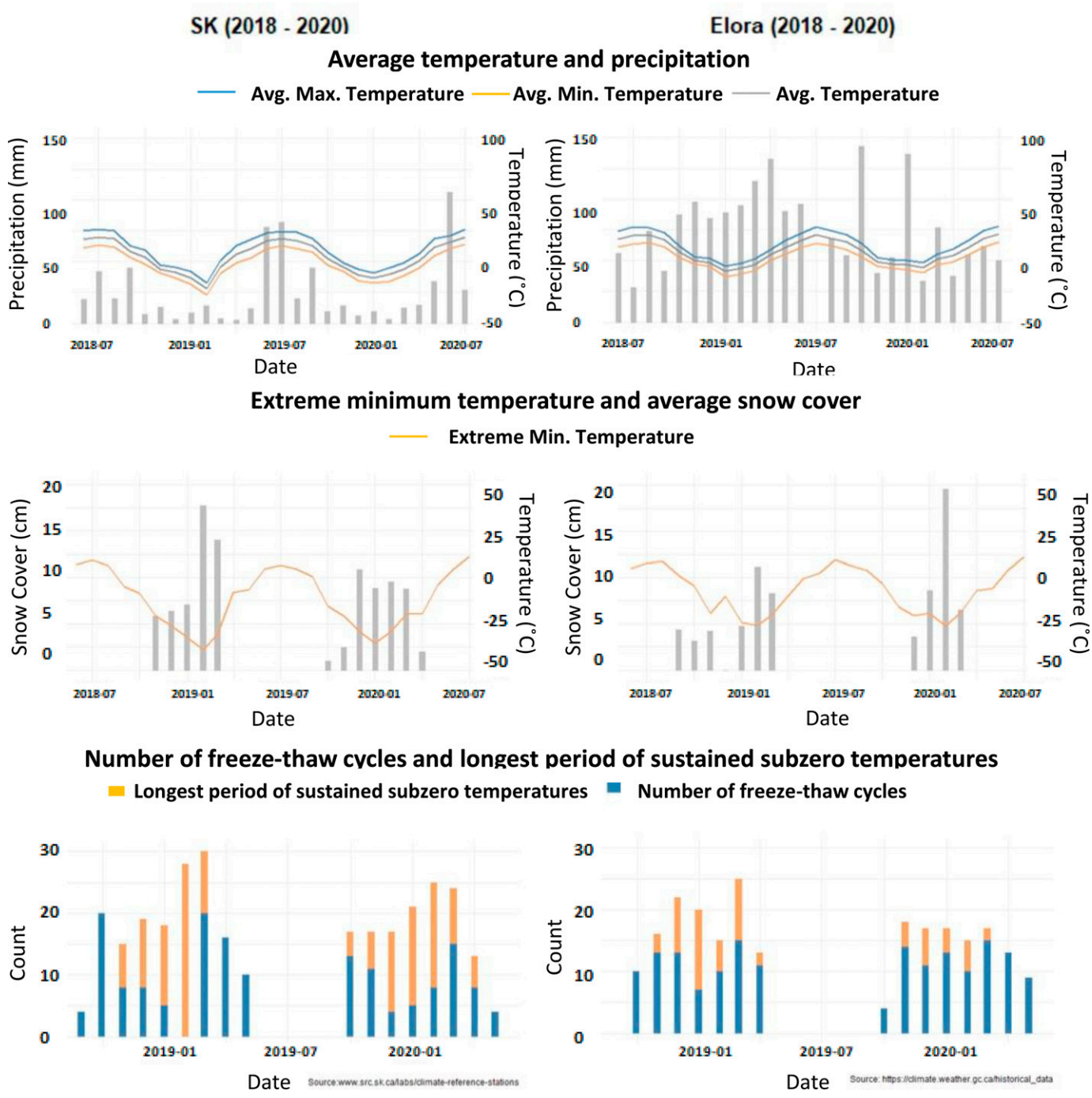

Supplemental Fig. 7. Climatic conditions in Saskatoon, SK, Canada (SK) and Elora, ON, Canada (Elora) from June 2018 to July 2020. The longest period of sustained sub-zero temperatures is given as a count of consecutive days with sustained sub-zero temperatures. Climatic data for SK were retrieved from the Saskatchewan Research Council Website at the Saskatoon Climate Reference Station, and climate data for Elora were retrieved from the Environment Canada Website for the Elora Research Station.

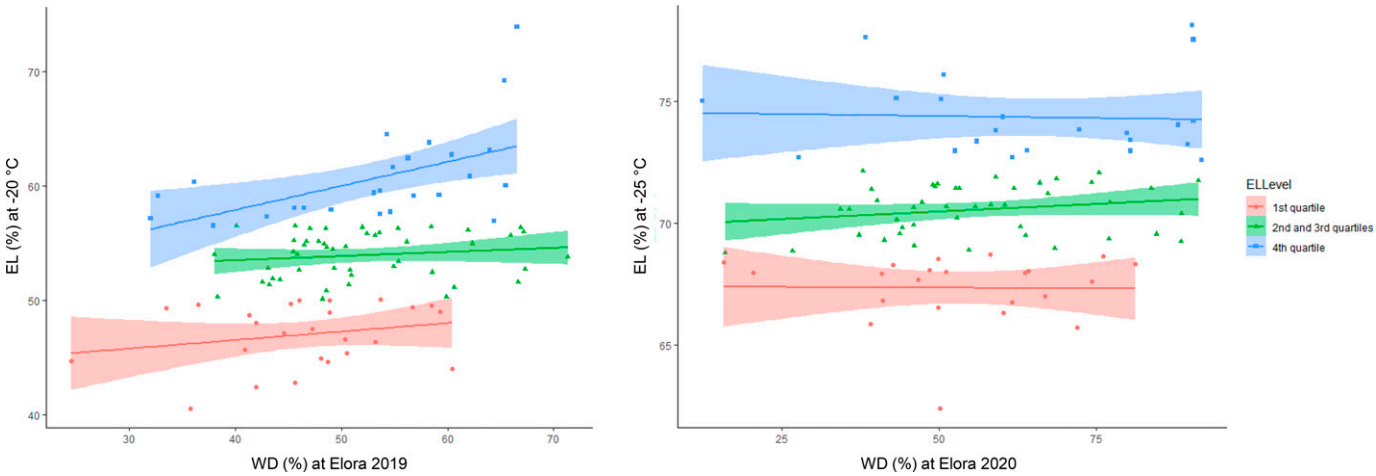

Supplemental Fig. 8. Relationship between best linear unbiased predictors (BLUPs) of electrolyte leakage (EL) and field winter damage (WD) in *Rosa* ×*hybrida*. WD was a measurement of cane dieback in the field using the following formula: WD $(\%) = 100 \times \frac{ld}{lt}$, with WD being the percentage of winter damage, ld the length of dieback, and lt the length of the whole cane. (**A**) EL (%) at −20 °C and BLUPs of WD collected at Elora, ON, Canada in 2019 (Elora 2019) in the mapping population CA60 × Singin' in the Rain ['SITR' ('MACivy')], (**B**) EL (%) at −25 °C and BLUPs of WD collected at Elora, ON, Canada in 2020 (Elora 2020) in the mapping population Easy Does It ['EDI' ('HARpageant')] × 'George Vancouver' ('GV'). Each data point corresponds to an individual. Genotypes were ranked based on EL at −20 °C for the CA60 × 'SITR' population, at −25 °C for the 'EDI' × 'GV' population. For both populations, individuals were grouped into three categories of electrolyte leakage according to their affiliation to either the first quartile of the distribution, the second and third quartiles, or the fourth quartile, and their level of freezing tolerance under artificial conditions was plotted against their level of field winter damage in (**A**) Elora 2019 for the 'CA60' × 'SITR' population, and (**B**) Elora 2020 for the 'EDI' × 'GV' population.

Supplemental Table 1. Field and electrolyte leakage (EL) data for 19 *Rosa ×hybrida* commercial cultivars and eight accessions used in Expt. 1, which aimed to determine the correlations between EL as an index of freezing tolerance and winterhardiness recorded in the field at different Canadian locations: Vineland, ON, Canada (VRIC); Saskatoon, SK, Canada (SK); and Olds, AB, Canada (OA).

Genotypes	Field data		Freezing experiments in artificial conditions						
				EL (%)					LT50
Cultivars	USDA cold hardiness zone (1–13 scale)	Field WH at VRIC (0–5 scale)[z]	Replications (no.)	−20 °C	−15 °C	−10 °C	−5 °C	Control	(°C)[y]
Cardinal Song (MEImouslin)	4	3	86.9	82.4	47.9	20.3	14.7	−11	
Caroline de Monaco (MEIpierar)	7	3	3	83.5	84	41.4	20	14.3	−11
Desert Peace (MEInomad)	7	3	1	75.2	71.4	20.3	16.2	13	−14
Gentle Giant (WEKrigoyelo)	6	4	1	94.5	91.8	27.7	14.1	13.6	−12
George Vancouver	3	1	1	72.3	63.3	20.2	25.7	19.9	−20
John Cabot	3	0.33	1	63.2	59.7	38.6	12.6	15.9	−15
John Davis	2	0	1	67.2	42.9	21.7	25	13.7	−17
John Franklin	3	3	77.9	54.8	22.8	24.1	14.8	−15	
Knock Out (RADrazz)	4	1	89.6	85.2	15.2	11.9	17.8		
Lambert Closse	3	2	3	80.1	75.4	39.4	14.1	11.3	−12
Peace	5	3	3	80.4	74.5	36.9	15.9	15.4	−13
Novalis (Poseidon)	6	2	77	54.2	21.6	23.5	15.2	−16	
Quadra	3	0	3	72.3	59.2	28.7	18.4	16.6	−15
Salmon Vigorosa (KORmuse)	5	2	76.6	81	53.1	15.8	16.9	−10	
Singin' in the Rain (MACivy)	6	4	1	86.4	88.7	82.6	19.2	18.9	−11
William Baffin	2	0	3	61.8	43.6	24.6	16.2	13.8	−18
Yellow Submarine (BAIine)	4	3	2	95.3	89.9	43.2	17.7	12.9	−10
Control		0.67	3	78	76.2	27.4	13.9	11.9	−13
CA60									

	Field WH at SK	Field WH at OA		EL (%)					LT50
	(0–5 scale)	(0–5 scale)	Replications (no.)	−20 °C	−15 °C	−10 °C	−5 °C	Control	(°C)
Selections									
S13–10	0.2	0	2	58.9	43.9	22.3	18.2	16.9	−19
S13–29	0.8	2	2	54.9	36.3	21.4	17.1	14.6	−22
S13–3	4.2	3	1	78.3	58.4	15.1	21.8	22.9	−15
S13–32	0.2	0	1	64.5	43.2	25.8	18.0	16.2	−18
S13–35	3.4	3	2	73.3	56.9	24.7	19.0	14.7	−15
S13–6	3.2	5	1	72.2	79.7	19.0	24.1	14.3	−14
S13–7	3.6	2	2	70.1	51.9	29.0	19.7	14.7	−16
S13–8	2	2	1	77	58.1	25.8	16.4	21.2	−16

[z]Winterhardiness (WH) was recorded on a scale from 0 to 5 (0 = no winter damage, 1 = damage on the tips of the canes only, 2 = damage down to the snow line, 3 = damage to the crown with good spring regrowth, 4 = damage to the crown with poor spring regrowth, 5 = dead plant).

[y]The lethal temperature for which 50% of the plants are dead (LT50) was estimated for each genotype using a logit model approach.

Supplemental Table 2. Generalized linear mixed model [GLMM (SAS version 9.4; SAS Institute Inc., Cary, NC)] of the effect of temperature (T), genotype (G), and replication (R) on the electrolyte leakage and index of injury measured in controlled conditions after freezing treatments with temperature tests ranging from −10 to −50°C for the *Rosa* ×*hybrida* genotypes CA60, Easy Does It™ ('HARpageant'), 'George Vancouver', and Singin' in the Rain™ ('MACivy').

1. Electrolyte leakage

Covariance parameters[z]	Subject	Estimate		
T × R		0		
G × T × R	Stem_section	0.05406		
Fixed effects	Numerator df	Denominator df	*F* value	*P* > *F*
T	3	9	210.15	<0.0001
G	1	171	1903.61	<0.0001
T × G	1	171	2.37	0.1259

2. Index of injury

Covariance parameters	Subject	Estimate		
T × R		0.004033		
G × T × R	Stem_section	0.08258		
Fixed effects	Numerator df	Denominator df	*F* value	*P* > *F*
T	8	9	82.16	<0.0001
G	3	167	84.98	<0.0001
T × G	24	167	2.76	<0.0001

[z]The data were analyzed with a beta distribution and a logit link function, and the model was used to compute the best linear unbiased estimators (BLUE) of electrolyte leakage using statistical software (SAS version 9.4).

Supplemental Table 3. Lethal temperature for which 50% of the plants are dead (LT50) for the *Rosa* ×*hybrida* genotypes CA60, Easy Does It™ ['EDI' ('HARpageant')], 'George Vancouver' ('GV'), and Singin' in the Rain™ ['SITR' ('MACivy')].

Label	LT50 (°C)[z]	SE	df	*t* value	*P* > *t*	Lower interval	Higher interval
LT50 CA60	−17	1.25	70			−20	−15
LT50 'SITR'	−14	0.69	70			−16	−13
Difference in |LT50 CA60| and |LT50 'SITR'|	3	1.08	70	2.67	0.0094		
LT50 'EDI'	−17	0.55	70			−18	−16
LT50 'GV'	−28	1.97	70			−31	−24
Difference in |LT50 'EDI'| and |LT50 'GV'|	11	175	70	6.21	<0.0001		
Difference in |LT50 'SITR'| and |LT50 'EDI'|	2	0.69	70	3.51	0.0008		
Difference in |LT50 'CA60'| and |LT50 'GV'|	10	1.52	70	6.98	<0.0001		

[z]The LT50 was estimated from nonlinear dosage response curves from the index of injury measured under controlled conditions using statistical software (SAS version 9.4; SAS Institute Inc., Cary, NC).

Supplemental Table 4. Generalized linear mixed model [GLMM (SAS version 9.4; SAS Institute Inc., Cary, NC) of the effect of temperature and genotype on the electrolyte leakage measured in controlled conditions after freezing treatments with temperature tests ranging from −10 to −20 °C for the *Rosa* ×*hybrida* population CA60 × Singin' in the Rain ['SITR' ('MACivy')] and from −15 to −40 °C for the population Easy Does It ['EDI' ('HARpageant')] × 'George Vancouver' ('GV').

1. CA60 × 'SITR' population

Covariance parameters[z]	Subject	Estimate		
Intercept	Genotype	0.02857		
Temperature	Genotype	0.008490		
Intercept	Replication	0.002808		
Temperature	Replication	0.004504		
Temperature × Genotype	Replication	0.08122		
Fixed effects	Numerator df	Denominator df	*F* value	$P > F$
Temperature	2	15	251.51	<0.0001

2. 'EDI' × 'GV' population

Covariance parameters	Subject	Estimate		
Intercept	Replication	0.03838		
Temperature	Replication	0.006010		
Intercept	Genotype	0.02795		
Temperature	Genotype	$1.11*10^{-12}$		
Fixed effects	Numerator df	Denominator df	*F* value	$P > F$
Temperature	5	10	136.40	<0.0001

[z]The data were analyzed with a beta distribution and a logit link function, and the model was used to compute the best linear unbiased prediction (BLUP) of electrolyte leakage.

Supplemental Table 5. Lethal temperature for which 50% of the plants are dead (LT50) estimated from nonlinear dosage response curve for the progeny of the *Rosa* ×*hybrida* population Easy Does It ['EDI' ('HARpageant')] × 'George Vancouver' ('GV').

Genotype	LT50 (°C)[z]	Genotype	LT50 (°C)	Genotype	LT50 (°C)	Genotype	LT50 (°C)
Above avg freezing tolerance			Avg freezing tolerance			Below avg freezing tolerance	
EDI.GV.60	−28	EDI.GV.13	−21	EDI.GV.28	−19	EDI.GV.104	−17
EDI.GV.10	−26	EDI.GV.43	−21	EDI.GV.36	−19	EDI.GV.21	−17
EDI.GV.24	−25	EDI.GV.47	−21	EDI.GV.41	−19	EDI.GV.3	−17
EDI.GV.37	−25	EDI.GV.79	−21	EDI.GV.44	−19	EDI.GV.35	−17
EDI.GV.39	−25	EDI.GV.90	−21	EDI.GV.51	−19	EDI.GV.68	−17
EDI.GV.42	−25	EDI.GV.93	−21	EDI.GV.53	−19	EDI.GV.88	−17
EDI.GV.5	−25	EDI.GV.106	−20	EDI.GV.7	−19	EDI.GV.22	−16
EDI.GV.8	−25	EDI.GV.15	−20	EDI.GV.72	−19	EDI.GV.33	−16
EDI.GV.17	−24	EDI.GV.34	−20	EDI.GV.73	−19	EDI.GV.54	−16
EDI.GV20	−24	EDI.GV.4	−20	EDI.GV.74	−19	EDI.GV.56	−16
EDI.GV.38	−24	EDI.GV.50	−20	EDI.GV.81	−19	EDI.GV.58	−16
EDI.GV.27	−23	EDI.GV.52	−20	EDI.GV.91	−19	EDI.GV.66	−16
EDI.GV.40	−23	EDI.GV.61	−20	EDI.GV.96	−19	EDI.GV.70	−16
EDI.GV.45	−23	EDI.GV.63	−20	EDI.GV.25	−18	EDI.GV.76	−16
EDI.GV.48	−23	EDI.GV.67	−20	EDI.GV.31	−18	EDI.GV.86	−16
EDI.GV.11	−22	EDI.GV.75	−20	EDI.GV.46	−18	EDI.GV.105	−15
EDI.GV.14	−22	EDI.GV.78	−20	EDI.GV.55	−18	EDI.GV.49	−15
EDI.GV.16	−22	EDI.GV.85	−20	EDI.GV.65	−18	EDI.GV.57	−15
EDI.GV.30	−22	EDI.GV.100	−19	EDI.GV.71	−18	EDI.GV.23	−15
EDI.GV.32	−22	EDI.GV.12	−19	EDI.GV.9	−18	EDI.GV.82	−15
EDI.GV.92	−22	EDI.GV.26	−19			EDI.GV.89	−15

[z]The LT50 was estimated from nonlinear dosage response curves from the index of injury measured under controlled conditions using statistical software (SAS version 9.4; SAS Institute Inc., Cary, NC).

Supplemental Table 6. Generalized linear mixed model [GLMM (SAS version 9.4; SAS Institute Inc., Cary, NC) of the effect of genotype and genotype × environment on winter damage for the *Rosa* ×*hybrida* mapping population CA60 × Singin' in the Rain™ ['SITR' ('MACivy')] across three environments: Elora, ON, Canada, in 2019 (Elora 2019) and 2020 (Elora 2020), and Saskatoon, SK, Canada (Sask 2019) and across individual environments, and for the *R.* ×*hybrida* mapping population Easy Does It™ ['EDI' ('HARpageant')] × 'George Vancouver' ('GV') across one environment: Elora, ON, Canada, in 2020 (Elora 2020).

		Tests of covariance parameters		
Covariance parameters[z]	Estimate	χ^2	$P > \chi^2$	Ratio Vge/Vg
1. CA60 × 'SITR' population				
Elora2019, Elora 2020, Sask 2019				
Environment	0.4264		<0.0001	1.33
Block (Environment)	0.08588		<0.0001	
Genotype	0.2390		<0.0001	
Genotype × Environment	0.3188		<0.0001	
Elora 2019				
Bloc	66.51			
Genotype	158.09	175.22	<0.0001	
Residual	160.73			
Elora 2020				
Bloc	12.6980			
Genotype	1.0654	316.37	<0.0001	
Sask 2019				
Bloc	0.01650			
Genotype		0.3156	84.73	<0.0001
2. 'EDI' × 'GV' population				
Bloc	0			
Genotype	1.2053	97.54	<0.0001	

[z]The data were analyzed separately for each population. At the exception of the data for the individual environment Elora 2019, the data were fitted to a beta distribution and a logit link function. Elora 2019 data were fitted to a Gaussian distribution. The models from individual locations were used to compute the best linear unbiased prediction (BLUP) of winter damage. The $\frac{Vge}{Vg}$ ratio was given to estimate the amount of variation due to the genotype × environment interaction relatively to the genotypic variance, with V_{ge} the variance associated with the genotype × environment interaction and V_g the genotypic variance.

Supplemental Table 7. Generalized linear mixed model [GLMM (SAS version 9.4; SAS Institute Inc., Cary, NC) of the effect of genotype and genotype × environment on regrowth for the *Rosa* ×*hybrida* mapping population CA60 × Singin' in the Rain™ ['SITR' ('MACivy')] across four environments: Elora, ON, Canada, in 2019 (Elora 2019) and 2020 (Elora 2020), and Saskatoon, SK, Canada, in 2019 (Sask 2019) and 2020 (Sask 2020) and across individual environments, and for the *R* ×*hybrida* mapping population Easy Does It™ ['EDI' ('HARPageant')] × 'George Vancouver' ('GV') across one environment (Elora 2020).

		Tests of covariance parameters		
Covariance parameters[z]	Estimate	χ^2	$P > \chi^2$	Vge/Vg ratio
1. CA60 × 'SITR' population				
Elora2019, Elora 2020, Sask 2019 and Sask 2020				
Environment	113		0.0013	3.09
Bloc(Environment)	52.6643		<0.0001	
Genotype	55.3091		0.0015	
Genotype × Environment	170.67		<0.0001	
Residual	839.70			
Elora 2019				
Bloc	0.001476			
Genotype	0.04041		<0.0001	
Residual	0.04457			
Elora 2020				
Bloc	0.000745			
Genotype	0.03012		<0.0001	
Residual	0.04377			
Sask 2019				
Bloc	0.006495			
Genotype	0.03274		<0.0001	
Residual	0.1129			
Sask 2020				
Bloc	0.002719			
Genotype	0.02542		0.003	
Residual	0.1435			
2. 'EDI' × 'GV' population				
Fixed effect	F value	$P > F$		
Cov_spline	6.98	<0.0001		
Covariance parameters	Estimate		Tests of covariance parameters	
		χ^2	$P > \chi^2$	
Genotype	0.05231	12.90	<0.0001	
Residual	0.14			

[z]The data were analyzed separately for each population. The data fitted a lognormal distribution and an identity link function. The data for the 'EDI' × 'GV' population were corrected for spatial variability using radial smoothing. The models from individual locations were used to compute the best linear unbiased prediction (BLUP) of regrowth. The $\frac{Vge}{Vg}$ ratio was given to estimate the amount of variation due to the genotype × environment interaction relatively to the genotypic variance, with V_{ge} the variance associated with the genotype × environment interaction and V_g the genotypic variance.

Supplemental Table 8. Evidence for the presence of C-binding repeat transcription factor (CBF/DREB) and Inducer of CBF expression (ICE1)-transcription factors on linkage groups (LGs) 1, 2, 3, and 7 of the reference genome *Rosa chinensis* 'Old Blush' homozygous v2.0.

Gene name	LG	Location	Description
RcHm_v2.0_Chr1g0376641	1	RcHm_v2.0_Chr1:63847494.63848870	*CBF4/DREB1D*
RcHm_v2.0_Chr3g0472361	3	RcHm_v2.0_Chr3:18244191.18245644	*CBF1/DREB1B*
RcHm_v2.0_Chr7g0199331	7	RcHm_v2.0_Chr7:17371406.17372131	*CBF4/ DREB1D*
RcHm_v2.0_Chr7g0199381	7	RcHm_v2.0_Chr7:17422407.17424183	*CBF3/DREB1A*
RcHm_v2.0_Chr2g0176421	2	RcHm_v2.0_Chr2:88244910.88247805	*ICE1*
RcHm_v2.0_Chr7g0188921	7	RcHm_v2.0_Chr7:8295405.8298561	*ICE1*